Floral Stage Optimization and Immune Evasion Enhance *Agrobacterium*-Mediated Genome Editing in *Arabidopsis*

Mao-Sen Liu[†], Teng-Kuei Huang[†], Yi-Chieh Wang, Si-Chong Wang, Chih-Hang Wu, Chih-Horng Kuo, Erh-Min Lai*

Institute of Plant and Microbial Biology, Academia Sinica, Taipei, Taiwan

*Correspondence (Tel: +886-2-2787-1158; email: emlai@gate.sinica.edu.tw)

[†]These authors contributed equally to this work

Author details, including affiliation and email address

msliu@gate.sinica.edu.tw; tengkueih@gmail.com; ejw@gate.sinica.edu.tw; sky972sakura@gmail.com; wuchh@gate.sinica.edu.tw; chk@gate.sinica.edu.tw; emlai@gate.sinica.edu.tw

ORCID ID

ORCID ID of the authors: M.-S.L. 0000-0003-0324-5866; T.-K.H. 0000-0001-7369-3678; S.-C.W. 0000-0002-6192-8844; C.-H.W. 0000-0003-1616-1872; C.-H.K. 0000-0002-2857-0529; E.-M.L. 0000-0003-3630-8683

ABSTRACT

Agrobacterium-mediated transformation via floral inoculation (AMT-FI) enables genetic engineering without tissue culture. It is widely used in the model plant *Arabidopsis thaliana*, yet its efficiency and broader applicability remain limited. Here, we identify key floral stages and develop novel strategies to enhance AMT-FI-based genome editing. Using a dual-reporter system (RUBY and hygromycin resistance), we determined that flowers opened at 6 days post-inoculation (DPI) are optimal for high transformation efficiency, with nearly 100% of siliques harboring transformants. However, *Agrobacterium* infection induced ovule abortion, particularly in wild-type (Col-0) plants, whereas *efr* mutants lacking the EF-Tu receptor (EFR)-mediated pattern-triggered immunity (PTI) showed reduced ovule abortion. Notably, *efr* mutants exhibited more RUBY-positive ovules and significantly enhanced genome editing efficiency, despite showing no improvement in stable transformation rates. These results suggest that PTI restricts transient transformation rather than T-DNA integration. We further engineered stealth *Agrobacterium* strains expressing a chimeric EF-Tu for evading recognition by EFR. These GV3101-derived strains, named as AS201 and AS202, enhanced both transient transformation and genome editing efficiency without significantly altering stable transformation frequency. Remarkably, genome-edited T1 plants could be recovered based on phenotype or direct sequencing without the need for antibiotic selection when targeting flowers opened at 6 DPI. Our findings reveal EFR-mediated immunity as a key barrier to efficient transient transformation and genome editing via AMT-FI. By integrating floral stage selection, immune evasion, and *Agrobacterium* engineering, this study provides a practical and versatile platform to advance plant genome engineering.

KEY WORDS

Arabidopsis, *Agrobacterium*, floral inoculation, plant immunity, genome editing, *Agrobacterium*-mediated transformation, EF-Tu, EFR

INTRODUCTION

Agrobacterium species are unique bacteria capable of cross-kingdom gene transfer, leading to diseases like crown gall or hairy root in a wide range of plant species (Hwang et al., 2017; Lacroix and Citovsky, 2019). This remarkable ability has been harnessed in plant genetic engineering by replacing the oncogenes within T-DNA region of tumor-inducing plasmids with genes of interest (Hooykaas, 2023; Suzuki et al., 2009). *Agrobacterium*-mediated transformation (AMT) has become a cornerstone technique in plant biology and the development of genetically modified organisms (GMOs) that stably express agricultural traits for crop improvements (Bevan, 1984; Gelvin, 2003).

Beyond enabling stable gene integration, AMT also supports transient expression of genome-editing machinery, allowing precise genome modifications. Since the T-DNA containing these editing components can be eliminated via chromosome segregation in subsequent generations, this strategy mitigates food safety concerns associated with GMOs (Pixley et al., 2022).

Agrobacterium naturally infects somatic plant cells by responding to wound signals in roots or stems. Interestingly, it can also target germline tissues such as female gametophytes, which laid the foundation for the floral dip method widely used in *Arabidopsis thaliana* (Angulo et al., 2023; Clough and Bent, 1998). This method, referred to as *Agrobacterium*-mediated transformation by floral inoculation (AMT-FI), bypasses labor-intensive tissue culture, offering a more efficient transformation pathway. However, its application in species beyond *A. thaliana* has limited success (Bélanger et al., 2024).

Although many plant factors that promote or suppress tumorigenesis and AMT have been identified, the genes involved in AMT-FI appear to be distinct (Hwang et al., 2017; Lacroix and Citovsky, 2019; Weisberg and Chang, 2023). Several *Arabidopsis* mutants or ecotypes resistant to root transformation remain susceptible to AMT-FI (Mysore et al., 2000; Nam et al., 1997). Notably, *polQ* mutants lacking DNA polymerase theta are completely deficient in T-DNA integration via AMT-FI but retain capability for stable transformation in roots, albeit at lower efficiencies (Nishizawa-Yokoi et al., 2021; van Kregten et al., 2016). These findings highlight fundamental mechanistic differences between AMT in germline and somatic cells. Understanding the genetic and molecular basis of AMT-FI is crucial to expanding its utility across plant species.

Plant immunity plays a pivotal role in suppressing tumorigenesis and AMT efficiencies (Dodds et al., 2024; Tiwari et al., 2022). Upon *Agrobacterium* infection, plants recognize pathogen-associated molecular patterns (PAMPs) such as EF-Tu, flagellin, and cold-shock proteins by pattern-recognition receptors (PRRs), activating pattern-triggered immunity (PTI) that suppress transformation (Fürst et al., 2020; Saur et al., 2016; Wang et al., 2018; Wu et al., 2014; Zipfel et al., 2006). Salicylic acid (SA) is a key defense hormone that reduces tumor formation and transient transformation (Anand et al.,

2008). Additionally, antimicrobial secondary metabolites, including glucosinolates and camalexin, restrict *Agrobacterium* infection at early and late stages, respectively (Shih et al., 2018). These defense strategies collectively highlight the resilience of plants to counteract *Agrobacterium* infection and limit its transformation success.

In *Arabidopsis*, the EF-Tu receptor (EFR) plays a key role in recognizing *Agrobacterium* EF-Tu and inhibiting transient transformation (Wang et al., 2018; Wu et al., 2014; Zipfel et al., 2006). However, the impact of EFR-mediated PTI on stable transformation remains obscure (van Tol et al., 2022). Moreover, its influence on AMT-FI-mediated genome editing has not been fully elucidated. Although a recent study used *A. thaliana efr* mutants to investigate this question, conclusive evidence is lacking (van Tol et al., 2022).

In this study, we investigated the temporal and spatial localization of *Agrobacterium* cells and transformation events during AMT-FI in *A. thaliana.* A dual reporter system, combining a visible RUBY marker with a hygromycin resistance marker, was utilized to identify the floral tissues and stages most susceptible to AMT. Furthermore, we examined the impact of EFR-mediated PTI in transformation and genome-editing efficiencies. Our results revealed that AMT events peak in flowers open at 6 days post-inoculation (DPI), with *efr* mutants exhibiting significantly higher genome editing efficiency than Col-0. Moreover, we engineered two independent *Agrobacterium* strains expressing a chimeric EF-Tu, which further enhanced both transient expression and genome editing efficiency without significantly altering stable transformation frequency. These findings offer new strategies to facilitate AMT-FI-based genome editing in plants.

RESULTS

Agrobacterium enters the female reproductive organ within one hour but transformation events occur in open flowers after five days post inoculation

Although transformation is thought to occur when the female gametophyte becomes accessible, direct links between floral stage and transformation success remain unclear. To investigate the spatial and temporal dynamics of *Agrobacterium* infection and transformation, we engineered a fluorescently labeled *Agrobacterium* strain for live tracking. *Agrobacterium* GV3101 carrying the disarmed Ti plasmid pMP90 (hereafter referred as GV3101), constitutively expressing GFP marker and a T-DNA expressed mCherry2, was used for floral inoculation in *A. thaliana* Col-0 (Fig.1a, 1b). GFP-expressing *Agrobacterium* cells were observed as early as 1 hour post-inoculation (HPI) in the early developmental stage of open gynoecia, the female reproductive organ lacking central placenta tissue (Fig. 1c) but were not detected in the later stage of gynoecia containing central placenta tissue (Fig. 1d). This implied that developing

placenta may act as a physical barrier to *Agrobacterium* entry during early infection. By 6 HPI, *Agrobacterium* cells accumulated in the locule of open gynoecia (Fig. 1e, 1f), whereas no signal was seen in closed gynoecia (Fig. 1g). This indicated that open gynoecia serve as the main entry point of *Agrobacterium* into the locule before development of female gametophyte.

At one day post-inoculation (DPI), *Agrobacterium* cells were detected in locules of younger, closed gynoecia (Fig. 1h) but were absent in older gynoecia undergoing ovule development (Fig. 1i). At 3 DPI, *Agrobacterium* persisted in the locules of more mature gynoecia (Fig. 1j), and at 5 DPI, just prior to floral open (anthesis), *Agrobacterium* cells were enriched around the micropyles , the ovular opening through which the pollen tube and possibly *Agrobacterium* gain access (Fig. 1k). Despite the sustained presence of *Agrobacterium*, successful T-DNA expression indicated by mCherry2 fluorescence was not detected before anthesis (Fig. 1c-k). Similarly, the RUBY reporter signal was absent in gynoecial tissues until after flower opening (Fig. 2c). Following anthesis, mCherry2 signals became visible in cells adjacent to the egg cell/zygote and in the micropyle region where *Agrobacterium* cells had accumulated (Fig. 1l, 1m). Transformation signals were also detected in the integument, the ovule's outer protective layer (Fig. 1m).

Together, these observations reveal that while *Agrobacterium* rapidly enters the open gynoecium as early as 1 HPI, transformation events are temporally restricted, becoming detectable only in open flowers from 5 DPI onward. This correlates with key developmental transitions in ovule accessibility and gametophyte maturity.

RUBY-based reporter system uncovers transformation dynamics and floral abnormalities

The current method for quantifying transformation efficiency of AMT-FI primarily relies on the use of antibiotic resistance genes, using survival rates of T1 seedlings as a proxy for transformation efficiency. However, this approach overlooks transient transformation events that occur at early stages post-inoculation. To better capture both the transient and stable transformation events, we developed a dual-reporter system combining the visible RUBY marker with a hygromycin resistance gene (Fig. 3a).

We first assessed the floral organs exhibiting RUBY expression. The earliest detection of RUBY signals was observed at 4 DPI, localized at the sepals of floral buds (Fig. 2a). By 5 DPI, RUBY expression appeared on the stigma of open flowers but not on pollen grains (Fig. 2b). Dissection of the ovaries revealed RUBY signal in the transmitting tissues (Fig. 2c), as well as in ovules and developing seeds (Fig. 2d, 2e). While many RUBY ovules were abortive (Fig. 2d), others continued to develop normally (Fig. 2e). Most flowers developed and opened normally (Fig. 2f) while a minor subset exhibited

developmental abnormalities. These included flowers with partially open petals (Fig. 2g) and those where only the gynoecium emerged from the sepals (Fig. 2h). In mature seeds, RUBY expression ranged in intensity from light pink to dark purple (Fig. 2i), indicating variable expression levels.

In the hygromycin resistance assay, although most hygromycin-resistant seedlings expressed RUBY, a few hygromycin-sensitive seedlings also showed weak RUBY signals (less than 1% of total transformants, Fig. 2j). Conversely, not all hygromycin-resistant seedlings exhibited uniform RUBY expression throughout the plants (Fig. 2k).

Collectively, the dual-reporter system offers a more comprehensive and sensitive tool for monitoring transformation events across the reproductive tissues. The RUBY reporter revealed that AMT-FI enables transformation in a variety of tissues within the female reproductive organ. However, it also uncovered associated developmental abnormalities in flowers and ovules, which in some cases prevent transformed ovules from developing into viable seeds.

Agrobacterium infection and EFR-mediated immunity synergistically disrupt ovule development

Since transformation events were only observed in ovaries after anthesis, we sought to trace the occurrence of AMT events in developing siliques using RUBY reporter as a marker (Fig. 3a). Flowers that opened between 1 to 10 DPI were labeled daily. Once embryos were fully developed, approximately 10 days after floral opening and pollination (Baud et al., 2002), each corresponding silique was examined for RUBY signals in ovules/developing seeds.

To assess the impact of EFR-mediated immunity on AMT-FI efficiency, we compared transformation efficiency in Col-0 wild-type (WT) plants and two EFR loss-of-function mutants (*efr*-1 and *efr*-2). Transformation events were primarily detected in flowers that opened between 5 to 9 DPI, with the highest frequency, nearly 100% of siliques showing RUBY-positive ovules in flowers opened at 6 DPI in both Col-0 WT and *efr* mutants (Fig 3b). The percentage of siliques harboring RUBY ovules did not differ significantly between WT and *efr*, suggesting that *Agrobacterium* can access the open gynoecium and subsequently transform ovules with comparable success across genotypes. However, the proportion of RUBY-positive ovules per silique was moderately higher in *efr* mutants, suggesting that compromising EFR-mediated PTI can enhance transformation efficiencies (Fig. 3c. Fig. S1a, S1b).

Given that AMT-FI often induced floral abnormalities and ovule abortion, we further investigated whether EFR-mediated PTI affects ovule viability. Strikingly, in Col-0 WT, nearly 60% of RUBY-positive ovules were abortive, indicating a strong negative impact of AMT-FI on ovule development. In *efr* mutants, although ovule abortion still occurred,

208 the rate was significantly reduced to ~45%. In contrast, fewer than 20% of non-RUBY
209 ovules were abortive, with no significant difference between Col-0 WT and *efr* mutants
210 (Fig. 3d). On average, *Agrobacterium* infection resulted in an ovule abortive rate of
211 ~35% (Fig. 3d, Fig. S1c).

212 Under normal growth conditions, ovule abortion rates are typically less than 1%(van Tol
213 et al., 2022), suggesting that the elevated abortion rates observed here are largely
214 attributable to *Agrobacterium* infection. While alleviation of EFR-mediated immunity
215 reduced the abortion rate among transformed ovules by ~15%, it did not restore ovule
216 viability to levels observed in non-transformed ovules (Fig. 3d). These findings suggest
217 that, in addition to EF-Tu PAMP recognition, other *Agrobacterium*-derived factors likely
218 contribute to ovule developmental disruption during AMT-FI.

219

220 **Temporal profiling reveals the optimal window for stable AMT-FI transformation**

221 Although the RUBY-positive ovules indicate transformation events, not all develop into
222 viable transgenic T1 seeds. To more accurately evaluate inherited transformation
223 efficiency, we quantified the number of viable transgenic seeds per silique and stable
224 transformation rate using hygromycin resistance (Hyg^R) as a selection marker. Stable
225 transformation efficiency was calculated based on the number and percentage of Hyg^R
226 seedlings collected daily from flowers opened at 5-9 DPI (Fig. 4).

227 As expected, siliques from flowers opened at 6 DPI exhibited the highest transformation
228 efficiency, with an average of ~90% and a peak at 100% of siliques containing Hyg^R
229 transformants (Fig. 4a). Consistently, stable transformation efficiency peaked at this
230 time point, with an average of ~26% and a peak at 40% (Fig. 4b). The number of T1
231 Hyg^R transformants per plant also reached its highest at 6 DPI, averaging ~55 and
232 peaking at 100 per plant (Fig. 4c).

233 These results highlight 6 DPI as the optimal floral stage for achieving the highest
234 frequency and efficiency of stable AMT-FI-mediated transformation in *Arabidopsis*.

235

236 **Trade-off between transformation and ovule development during AMT-FI**

237 Notably, a strong negative correlation was observed between transformation rate and
238 seed viability. Flowers that opened at 6 DPI, despite showing the highest AMT-FI
239 efficiency, produced lower number of viable seeds (Fig. 4d), likely due to the high
240 abortion rate of RUBY-positive ovules (Fig. 3d). However, *efr* mutants produced
241 significantly more viable seeds per silique from flowers that opened at 5 to 7 DPI (Fig.
242 4d), supporting a role for EFR-mediated immunity in transformation-associated ovule
243 abortion.

To determine whether the increased number of viable seeds per silique in *efr* mutants is a consequence of AMT-FI, we quantified seed production in plants treated with infiltration medium, and those inoculated with *Agrobacterium* GV3101 (Fig. S2). Under both conditions, *efr* mutants produced more seeds per silique than Col-0 WT (Fig. S2a, S2b). However, *Agrobacterium* infection further reduced seed numbers in both genotypes. To assess seed viability, we evaluated germination rates. Seeds from plants treated with infiltration medium germinated at nearly 100% in both Col-0 and *efr* but the germination rate is reduced (~90%) with *Agrobacterium* infection.

Collectively, these results suggest that EFR-mediated immunity may reduce seed output but pathogen-induced stress from *Agrobacterium* infection has a more substantial negative impact on seed viability than EFR alone. Suppressing EFR-mediated immunity improves seed viability but does not substantially alter stable transformation outcomes, highlighting a trade-off between transformation efficiency and ovule developmental success during AMT-FI.

EFR-mediated immunity suppresses genome editing efficiency

Although no significant increase in stable transformation efficiency was observed in *efr* mutants compared to Col-0 WT (Fig. 3c), previous studies have shown that *efr* mutants exhibit enhanced *Agrobacterium*-mediated transient expression (Zipfel et al., 2006; Wu, Liu et al., 2014). Since transient expression of CRISPR/Cas9 components is sufficient to induce genome editing without stable T-DNA integration, we next investigated the role of EFR-mediated immunity in regulating gene editing efficiency during AMT-FI.

W constructed a T-DNA vector carrying dual selection markers: a hygromycin resistance gene for selecting transgenic plants and a CRISPR/Cas9 system targeting the *ALS* gene, which confers dominant herbicide resistance (Chen et al., 2017), for identifying genome-edited plants (Fig. 5a). Given that the egg-cell is a major target of AMT-FI (Desfeux et al., 2000), we adopted a strategy that enables editing in monoploid germline cells at early developmental stages. Specifically, we applied an egg-cell-specific promoter previously shown to induce heritable mutations in the T1 generation (Wang et al., 2015). To enhance genome editing efficiency and streamline the screening process, we employed an A3A/Y130F-CBE_V01 base editor (termed as A3A-CBE in this study), which has demonstrated efficient C-to-T base editing in both rice and *Arabidopsis* under a ubiquitin promoter (Ren et al., 2021).

Using this construct, we transformed Col-0 WT and *efr* mutants and assessed T1 progeny for T-DNA integration (via hygromycin resistance) and genome editing (via tribenuron resistance conferred by *ALS* editing). The A3A-CBE system achieved an overall editing frequency of approximately 0.5% in total T1 seeds and about 20% among transformed individuals in the Col-0 WT background (Fig. 5b). Both *efr*-1 and *efr*-2

mutants showed higher editing rates, despite the increase was statistically significant only in *efr*-2. We also evaluated stable transformation efficiency by sowing T1 seeds on a hygromycin-containing medium but no significant increase can be observed in *efr* mutants (Fig. 5c).

To further validate these findings, we targeted *CLA1* and *PDS3*, two genes that cause albino phenotypes when biallelically edited (Liu et al., 2022). T1 seeds were germinated on a hygromycin-containing medium, and the numbers of green and albino seedlings were quantified (Fig. 5d). We observed a slight but consistent increase in the proportion of albino seedlings in *efr*-1 compared to Col-0 WT, supporting the conclusion that EFR-mediated immunity suppresses genome editing efficiency during AMT-FI.

Modification of *Agrobacterium* EF-Tu enhances transient gene expression and genome editing efficiency but not stable T-DNA integration efficiency

To further validate the role of EFR in suppressing genome editing efficiency during AMT-FI, we tested whether an *Agrobacterium* strain that evades EFR recognition mediates increased genome editing efficiency. To achieve this, we engineered *Agrobacterium* to express a modified EF-Tu incapable of triggering EFR-mediated PTI. *Agrobacterium* GV3101 possesses two EF-Tu-encoding genes, *tufA and tufB*, which produce a translation elongation factor. Our initial attempts to delete both *tuf* genes were unsuccessful, likely due to their essential function. However, a recent study demonstrated that replacing the entire or N-terminal region (amino acids 1-15) of *Agrobacterium* EF-Tu with that of *Pseudomonas syringae* pv. *tomato* (*Pst*) DC3000 reduced PTI activation and improved transient expression efficiency in *A. thaliana* leaves (Yang et al., 2023).

Using a similar concept but a different experimental approach, we engineered GV3101 by replacing amino acids 4-15 of both *tufA* and *tufB* with the corresponding region from *Pst* EF-Tu, referred to as $tufAB^{Pst4\text{-}15}$ (Fig. 6a). We generated two independent $tufAB^{Pst4\text{-}15}$ strains, named as AS201 and AS202, and compared them to the parental GV3101 strain for transient expression, genome editing and stable transformation efficiencies. To assess transient transformation, we transformed *A. thaliana* seedlings for transient expression analysis using a T-DNA-encoded GUS reporter (Wu et al., 2014). Both AS201 and AS202 showed significantly higher transient GUS activity in Col-0 WT compared to GV3101 (Fig. 6b, 6c). As expected, GV3101 exhibited ~20-fold higher GUS activity in *efr*-1 than in Col-0 due to the absence of EF-Tu recognition. However, in *efr*-1, AS201 and AS202 exhibited lower GUS activity than GV3101, indicating that the engineered EF-Tu proteins may compromise transformation efficiency when PTI is not a barrier for infection.

Encouraged by these results, we next tested whether the $tufAB^{Pst4\text{-}15}$ strains could improve genome editing efficiencies in Col-0 by AMT-FI. Compared to GV3101, both AS201 and AS202 significantly enhanced genome editing rates and produced more

edited T1 plants (Fig. 6d). As expected, we observed no significant difference in T-DNA integration rates or in the total number of transgenic T1 plants (Fig. 6e).

Sequencing-based screening of genome-edited plants

Our floral inoculation analysis demonstrated that flowers opened at 6 DPI showed a stable transformation efficiency ~26% (Fig. 4b). Based on this high efficiency, we reasoned that it may be possible to recover genome-edited T1 plants without prior selection of T-DNA integration step (Fig. 7a).

To test this, we targeted *CLA1* gene, which allows easy identification of edited plants based on their albino phenotype, complemented by sequencing analysis. We germinated T1 seeds from Col-0 and *efr* mutants on MS medium without hygromycin selection. Among these seedlings, we observed biallelically edited albino plants at the frequencies of 3.3% in Col-0, 3.7% in *efr*-1, and 4.2% in *efr*-2. We also identified green seedings carrying monoallelic edits, identified by Sanger sequencing. Their editing rates were 1.6% in Col-0, 15.9% in *efr*-1, and 4.7% in *efr*-2 (Fig. 7b). To further validate this strategy, we targeted the *ALS* gene without applying tribenuron selection. Among the T1 seedlings, we identified one edited plant out of 94 T1 seedlings from GV3101 and two out of 93 from $tufAB^{Pst4\text{-}15}$ mutant, AS201. All three edited T1 plants carried C-to-T base editing at the Pro197 locus, consistent with the expected *ALS* editing outcome (Fig. 7b).

In conclusion, genome-edited T1 plants can be obtained without prior selection for T-DNA integrated plants when screening seeds from flowers opened at 6 DPI. Furthermore, evading EFR-mediated PTI enhances genome editing efficiency, further supporting the role of plant immunity in constraining *Agrobacterium*-based genome engineering.

DISCUSSION

In this study, we provide mechanistic and practical insights into the *Agrobacterium*-mediated floral transformation process. By tracking transformation events with a dual-reporter system, we identified the optimal transformation window, leading to the success in obtaining edited plants without prior selection of T-DNA integration. Our findings also reveal EFR-mediated immunity as a key barrier to efficient transient transformation and genome editing via AMT-FI. By integrating floral stage selection, immune evasion, and *Agrobacterium* engineering, this study provides a versatile platform to advance plant genome engineering.

Different cell types exhibit varying susceptibility to *Agrobacterium* infection

Using RUBY as a T-DNA reporter, we detected strong RUBY signals in sepal, transmitting tissues, ovules, and developing seeds (Fig. 2). Notably, no RUBY signals were detected in pollen grains, consistent with earlier findings using GUS reporter (Ye et al., 1999). The variation in transformation efficiency likely reflects cell-type specific susceptibility to *Agrobacterium* infection or differential transcriptional activity of the CaMV 35S promoter (Kiselev et al., 2021). Additionally, we observed diverse RUBY expression patterns among hygromycin-resistant transgenic plants. Some plants expressed RUBY throughout their life cycle, while others showed expression only during seedling stages or specific organs. This variability may result from positional effects of T-DNA integration site or differences in promoter activity (Gelvin, 2003; Roca Paixao and Deleris, 2024). The presence of hygromycin-sensitive but RUBY-positive seedlings also suggests a possible truncation of the T-DNA at the left border (Fig. 3a), where the hygromycin resistance cassette is located.

Temporal and spatial tracking of *Agrobacterium* entry and transformation

Although various floral tissues and cell types can be transformed (Fig. 1, 2), only female gametes serve as heritable targets for producing progenies in *Arabidopsis* (Bechtold et al., 2000; Desfeux et al., 2000; Ye et al., 1999). Therefore, *Agrobacterium* entry into the locule of developing gynoecium is a crucial step in successful transformation (Desfeux et al., 2000).

Our data show that *Agrobacterium* enters the locule of open gynoecium within hours, colonizes reproductive tissues, and persists around the micropyle of ovules, potentially enabling transformation of egg cells and surrounding tissues. Despite early colonization, transformation events in gynoecium cells only occur in open flowers from 5 DPI onward, coinciding with floral opening and micropyle exposure.

Transient T-DNA expression can be observed as early as 1 DPI and highly abundant at 2 DPI when transforming somatic cells like leaves, seedlings, and root explants (Gelvin, 2003; Lopez-Agudelo et al., 2024; Wu et al., 2014). The delayed expression in germ cells may reflect differences in promoter activity, cell-type susceptibility, or route of *Agrobacterium* entry. Given that pollen tubes access ovules via the micropyle only after floral opening, they may serve as important carriers, facilitating *Agrobacterium* entry into ovules for transformation. Once inside, *Agrobacterium* could associate with male gametes or directly attach to egg cells for T-DNA transfer during fertilization. This proposed mechanism explains the high AMT-FI efficiency observed in flowers opening at 5-9 DPI and suggests that transformation occurs in young floral buds 5-9 days before anthesis, supporting previous findings (Clough and Bent, 1998; Desfeux et al., 2000; Ye et al., 1999).

395 **AMT peaks in flowers opened at 6 DPI and negatively correlate with seed viability**

396 Tracking transformation events by fluorescent marker revealed *Agrobacterium* targets
397 integument cells, egg cells and central cells for transformation (Fig. 1l, 1m), consistent
398 with previous findings (Bechtold et al., 2003). However, only the transformed egg cells
399 contribute to transgene inheritance. This explains why RUBY-based transformation
400 rates are significantly higher than those determined by hygromycin resistance (Fig. 3c,
401 4b). The use of the RUBY reporter enabled the discovery of floral stages accessible for
402 AMT-FI, revealing that nearly all ovaries from flowers open at 6 DPI were transformed,
403 yielding averaged an 26% stable Hyg^R T1 progeny. However, high transformation rates
404 were accompanied by increased ovule abortion, resulting in fewer viable seeds (Figs.
405 3d, 4b, 4d). In contrast, *efr* mutants exhibited lower abortion rates and higher seed
406 viability per silique, suggesting that EFR-triggered immunity contributes to
407 transformation-induced ovule loss. Evading plant immune responses could therefore
408 enhance the efficiency of transgenic seed production via AMT-FI.

409

410 **Evasion of EFR-mediated immunity enhances genome editing efficiency but not**
411 **stable transformation**

412 Although EFR-mediated immunity was discovered nearly two decades ago (Zipfel et al.,
413 2006), its influence on stable transformation and genome editing remain unclear. While
414 *efr*-1 mutants showed no improvement on gene targeting or stable transformation
415 efficiencies (van Tol et al., 2022), they do exhibit enhanced transient expression (Zipfel
416 et al., 2006; Wu, Liu et al., 2014; Yang et al., 2023). Our results confirm higher RUBY
417 transformation rates in *efr* ovules, but no significant increase in stable transformation
418 measured by hygromycin resistance (Figs. 4b, 6e).

419 However, we showed that genome editing efficiencies were significantly higher in *efr*
420 mutants and in Col-0 WT inoculated with the two engineered GV3101::$tufAB^{Pst4\text{-}15}$ strain,
421 AS201 and AS202 (Figs. 5, 6). This suggests that genome editing can be decoupled
422 from T-DNA integration. This is further supported by evidence that genome-edited
423 plants were successfully obtained from the *teb-5* (*polQ)* mutant, whereas T-DNA
424 integrated plants were not (van Tol et al., 2022). Thus, we proposed that enhancement
425 of editing efficiencies may result from higher transient expression of CRISPR/Cas9 in
426 egg cells in the absence of EFR-triggered immunity. Moreover, because editing can
427 occur without DNA integration (e.g., via ribonucleoprotein delivery), it may serve as a
428 proxy for measuring transgene expression levels in germline cells.

429

430 **Innovative strategies for enhancing genome editing efficiency**

Precision editing is critical for inducing dominant phenotypes by targeting an endogenous gene. However, current methods exhibit low efficiency compared to mutagenesis by Cas9 nuclease (Huang and Puchta, 2021). To overcome these limitations, we used an improved A3A-CBE base editor and achieved a high editing-to-integration ratio (~0.2) (Fig. 5). This construct, together with our optimized screening workflow, enables efficient dissection factors that influence stable transformation and genome editing efficiency in *Arabidopsis*.

Several recent studies have introduced innovative approaches to enhance stable transformation and genome editing. These include engineering of *Agrobacterium* strains to deliver type III secretion system effectors, T-DNA concatenation, and vector copy number manipulation (Dickinson et al., 2023; Raman et al., 2022; Szarzanowicz et al., 2024). Our success in engineering *Agrobacterium* strains with modified EF-Tu to evade EFR recognition, significantly enhanced genome editing efficiency. This reinforces the idea that boosting transient gene expression is a key determinant for successful genome modification via CRISPR/Cas9.

Despite native EFR is specific to Brassicaceae, several non-Brassicaceae crops have been engineered to express EFR for disease resistance (Boschi et al., 2017; Kunwar et al., 2018; Lu et al., 2015; Piazza et al., 2021; Schwessinger et al., 2015). These transgenic plants may show reduced *Agrobacterium*-mediated transformation. Our engineered GV3101::*tufAB*$^{Pst4\text{-}15}$ strains could overcome this limitation. Beyond EF-Tu, other *Agrobacterium*-derived PAMPs such as translation initiation factor IF1, cold-shock protein, and flagellin also trigger PTI via distinct receptors in different species (Fan et al., 2022; Fürst et al., 2020; Saur et al., 2016). This work sets the stage for the development of multi-modified *Agrobacterium* strains with broad compatibility, offering a roadmap to enhance AMT across diverse plant taxa.

EXPERIMENTAL PROCEDURES

Plant materials and growth condition

Arabidopsis thaliana Col-0, EF-Tu receptor (EFR) mutants, *efr*-1 (SALK_044334) and *efr*-2 (SALK_068675) were used in this study. Seeds were sown in soil (peatmoss:vermiculite:perlite = 12:1:1), germinated, and grown in a growth room under conditions of 22 °C with 16h light/8h dark photoperiod.

Bacterial growth condition

For tracking *Agrobacterium* localization and transformation events, *Agrobacterium* cells were cultured in 523 with appropriate antibiotics (Kado and Heskett, 1970). For genome editing experiments, LB medium supplemented with appropriate antibiotics was used. Freshly streaked out *Agrobacterium* colonies grown on 523 or LB agar were cultured in

469 the same medium (5 mL) for 2 days at 28 °C. The cultures were subsequently diluted
470 1:1000 in 50 mL 523 or LB, grown for 22-24 hours, harvested by centrifugation at 6000x
471 g for 20 minutes. The cell pellets were resuspended in infiltration medium (1/2 MS, 5%
472 sucrose, 0.04% silwet-L77, 44 nM BAP and 200 μM AS, pH=5.7) to OD_{600}=1.

473 **Plasmid construction**

474 Plasmid and primer information are listed in Table S1 and S2, respective. 35S::RUBY
475 plasmid (Addgene#160908) which provided a visible RUBY reporter and hygromycin
476 resistance reporter was obtained from Addgene.

477 The gentamycin resistance gene (Gen^R) of pRL662-GFP(S65T) (Yu et al., 2021) was
478 replaced by spectinomycin resistance gene from 35S::RUBY to obtain pRL662-
479 GFP(S65T)/Spe^R by use of Gibson Assembly® Master Mix (New England Biolabs, USA).
480 mCherry2 with a 3'-end nuclear localization signal (mCherry-NLS) was generated from
481 pEB2-2ndVal mCherry2-L (Addgene#104027) by PCR. PCR was performed by use of
482 KAPA HiFi HotStart ReadyMix PCR Kit (KapaBiosystems, South Africa) and PCR
483 products were cloned into the pJet1.2/blunt plasmid following the user manual of
484 CloneJET PCR Cloning Kit (ThermoFisher Scientific, USA). 35S::mCherry2-SV40/Kan^R
485 binary vector was constructed with Golden Gate Assembly.

486 A3A-CBE coding region was amplified from pYPQ265E2 (Addgene #164719) and was
487 subcloned into XbaI/SacI digested pHEE901 (Addgene #91707) via Gibson Assembly.
488 Protospacers were cloned into pA3A-CBE vectors as previously described (Steinert et
489 al., 2015). To generate the *tufAB*$^{Pst4-15}$ mutants in GV3101, we employed double
490 crossover vector using pEML041003-tufAPst4-15 and pEML41003-tufBPst4-15. Two
491 2.5-kb DNA fragment of modified *tufA* and *tufB* were amplified by two pairs of primers,
492 and cloned into pEML041003 by BsaI digestion. AS201 was generated by modifying
493 *tufB* followed by *tufA*, while AS202 was *tufA* followed by *tufB*. In both constructs, the
494 amino acids at positions 4-15 of EF-Tu were substituted from the native sequence
495 SKFERNKPHVNI to the *Pseudomonas syringae* variant EKFDRSLPHCNV.

496

497 **Seedling transient transformation and GUS activity assays**

498 *A. thaliana* seedling transient expression assay was performed by the AGROBEST
499 (*Agrobacterium*-mediated enhanced seedling transformation) method as previously
500 described, with minor modification (Wu et al., 2014). *Agrobacterium* cultures were
501 adjusted to an OD_{600}=0.01 in AB-MES medium for co-culture with seedlings. Infected
502 seedlings were collected for GUS activity assays after 2.5 days post-inoculation.

503

504 ***Agrobacterium*-mediated transformation by floral inoculation (AMT-FI)**

505 AMT-FI was performed according to the published procedure (Clough and Bent, 1998)
506 with modifications. For tracking *Agrobacterium* cells and transformation events, each
507 *Arabidopsis* plant was grown in a small pot (5 cm upper diameter x 5 cm high x 3.5 cm
508 bottom diameter). For genome editing experiments, three plants were grown in a large
509 pot (7.8 cm upper diameter x 7.8 cm high x 5.7 cm bottom diameter). Plants were grown
510 until they reached ~5 weeks old, with primary inflorescences reaching 10 to 15 cm tall.
511 The primary inflorescence was then removed to promote the emergence of secondary
512 inflorescences over the next 5 to 6 days. Immediately prior to floral dipping, all open
513 flowers were removed. Plants were submerged in *Agrobacterium*-containing infiltration
514 medium for 40 seconds, then laid horizontally in trays, covered with plastic film to
515 maintain high humidity, kept in the dark and incubated for 20 to 24 hrs. Plants were
516 returned to the growth room under the same growth condition.

517 For time-course experiments, newly opened flowers were labeled daily following
518 inoculation. GFP-labeled *Agrobacterium* cells and mCherry2 T-DNA reporter signals
519 were examined in ovaries using a Zeiss LSM 510 Meta confocal microscope

520 RUBY signals were monitored visually in plants transformed with GV3101 carrying the
521 35S::RUBY construct, assisted by a stereo microscope. A Zeiss Lumar V12 stereo
522 fluorescent microscope was used to capture images of floral organs, developing ovules,
523 seeds, and seedlings.

524 To evaluate AMT-FI efficiency by RUBY marker, siliques from RUBY-transformed plants
525 were collected daily. To assess stable transformation efficiency, seeds were sterilized in
526 70% ethanol for 10 min and plated on a 1/2 MS medium supplemented with 25 mg/L
527 hygromycin. The number of germinated seedlings and Hyg^R seedlings was recorded.
528 AMT-FI efficiency was determined based on the proportion of Hyg^R seedlings relative to
529 the total number of germinated seedlings.

530

531 **Assessment of genome editing efficiency**

532 To simultaneously measure the genome editing and AMT-FI efficiency, seeds from
533 plants transformed with a binary vector carrying a T-DNA-encoded base editor, a
534 sgRNA and a hygromycin resistance gene were surface sterilized and germinated on a
535 1/2 MS medium supplemented with either 5 mg/L tribenuron or 25 mg/L hygromycin,
536 both containing 100 mg/L timentin. After seven days, the numbers of tribenuron-
537 resistant, hygromycin-resistant, and albino T1 seedlings were recorded. AMT-FI
538 efficiency was estimated using a weight-based approach, assuming 10 mg of seeds
539 equals approximately 500 seeds.

540

541 **Statistical analysis**

542 An unpaired two-tailed Student's *t*-test, performed using GraphPad Prism 10, was used
543 to assess statistical differences either between Col-0 WT and *efr* mutants or across
544 time-course datasets.

545

546 **Author contributions**

547 M.-S.L, T.-K.H., C.-H. K. and E.-M.L, contributed to the conceptualization of the project.
548 M.-S.L. designed and performed AMT-FI. T.-K.H. designed and performed the genome
549 editing assay. M.-S.L., T.-K.H., Y.-C.W. and S.-C.W. performed experiments and
550 analyzed data. M.-S.L., T.-K.H., and E.-M.L. wrote the initial manuscript. E.-M.L., C.-H.
551 K. and C.-H.W. supervised the project. All authors reviewed and edited the manuscript.

552

553 **Acknowledgements**

554 The authors acknowledge the members of the Lai, Kuo, and Wu labs for discussion and
555 suggestion. We also thank the technical assistance of Live Cell Imaging Core Lab and
556 Sanger DNA sequencing service provided by Genomic Technology Core located at the
557 Institute of Plant and Microbial Biology, Academia Sinica. The funding was supported by
558 the Academia Sinica Grand Challenge Program (AS-GC-111-L02) to E.-M.L., C.-H. K.
559 and C.-H.W, and the intramural fund of the Institute of Plant and Microbial Biology,
560 Academia Sinica.

561

562 **Supporting Information**

563 Table S1. Plasmid information

564 Table S2. Primer list

565

566 **Conflict of interest statement**

567 The authors declare no conflict of interest.

568

569 **FIGURE LEGENDS**

570

571 **Figure 1. *Agrobacterium* enter open gynoecium within 1 hour but transformation**
572 **events occur in open flowers after 5 days post inoculation**

573 *Agrobacterium* GV3101 carrying pRL662-eGFP(S65T)/Spe^R and the binary vector
574 35S::mCherry2-NLS was used for floral inoculation on *Arabidopsis thaliana* Col-0 to
575 visualize *Agrobacterium* localization and transformation events (a). Schematic
576 illustration of the structure and development of gynoecium from early to mature stage
577 with stigma, style, ovary containing ovules (b).

578 After one hour post-inoculation (HPI), *Agrobacterium* cells had already entered the
579 locule of developing gynoecium (c) but were absent in later-stage gynoecia containing
580 developed placenta tissue (d). Between 6-9 HPI, more *Agrobacterium* cells were
581 observed in the locule (e), even at it began to close (f). *Agrobacterium* was not detected
582 in fully closed gynoecia (g).

583 At one day post-inoculation (DPI), *Agrobacterium* cells were detected in young closed
584 ovaries (h) but not in older ovaries undergoing ovule development (i). At 3 DPI (j),
585 *Agrobacterium* cells persisted in ovaries at late developmental stages. By 5 DPI,
586 *Agrobacterium* cells were enriched around the micropyle (arrow) (k), though no
587 mCherry2 signal was detected. At floral open stage after 6 DPI, *Agrobacterium*
588 accumulated around the micropyle, and mCherry2 signal became visible (l and m).

589 Asterisks (*) indicate placenta tissue; arrowheads denote developing ovule; arrows
590 indicate *Agrobacterium* located around micropyle. Panels (a to k) were merged channel
591 images; panels (l and m) show GFP, mCherry2, DIC and merged views. Scale bar= 100
592 μm.

593

594 **Figure 2. RUBY marker revealed transformation events in floral organs and**
595 **female tissues**

596 RUBY signals were observed in flowers (a), specifically on the stigma but not on pollen
597 grains (b), and in the transmitting tissue (c). In siliques, RUBY expression was detected
598 in both abortive (d) and developing ovules (e).

599 Flower morphology after AMT-FI ranged from normal open flowers (f) to partially open
600 flowers (g), and flowers with only gynoecia emerging from sepals (h), all with visible
601 RUBY signals.

602 RUBY signal intensity varied among seeds (i) and plants (j, k). (j) At the seedling
603 stage, hygromycin resistant (Hyg^R) and RUBY-positive seedling (left), non-transgenic
604 seedling (middle), and RUBY-positive but hygromycin sensitive (Hyg^S) seedling (right)

were observed. (k) Transgenic T1 plants with variable RUBY expression patterns from strong whole-plant expression to undetectable signal. Scale bar = 200 μm.

Figure 3. *Agrobacterium* infection and EFR-mediated immunity exert negative impacts on ovule development

(a) Experimental design: a schematic diagram illustrates the 35S::RUBY construct and experimental workflow. Transformation efficiency was evaluated based on the presence of RUBY-positive ovules and hygromycin-resistant seedlings.

(b) Percentage of siliques with RUBY-positive ovules recorded daily for Col-0 WT, *efr*-1, and *efr*-2 from flowers that opened at 1-10 DPI. Data are mean ± SD of three biological replicates from representative of two independent experiments.

(c) RUBY-based transformation. Percentage of RUBY-positive ovules (include both developed and abortive ovules) per silique collected from flowers of Col-0 WT, *efr*-1 and *efr*-2 opened at 5-9 DPI was calculated (all data points shown in Fig. S2a). Data are mean ± SD of averaged percentage of RUBY-positive ovules from three independent experiments (circle, triangle and rhombus symbols). Statistically significant differences ($p < 0.05$) between Col-0 WT and *efr* mutants are indicated.

(d) Ovule abortion rate. The abortion rate of RUBY-positive, non-RUBY, and total ovules per silique collected from flowers of Col-0 WT, *efr*-1 and *efr*-2 opened at 5-9 DPI was calculated (all data points shown in Fig. S2c). Data are mean ± SD of averaged abortion rate from three independent experiments (circle, triangle and rhombus symbols). Statistically significant differences ($p < 0.05$) between Col-0 WT and *efr* mutants are indicated.

Figure 4. AMT events occur mainly in flowers opened at 5-9 DPI, peaking at 6 DPI

Siliques and seeds developed from flowers that opened at 5-9 DPI in Col-0 WT, *efr*-1 and *efr*-2 mutants were analyzed through hygromycin resistance (Hyg^R) screening (a, b, c) and viability (d). Data are (a) percentage of siliques containing Hyg^R transformants, (b) percentage of Hyg^R transformants per silique, (c) number of Hyg^R transformants per plant, and (d) number of viable seeds per silique. Data are mean ± SD of six biological replicates from two independent experiments (circle and triangle symbols). Statistically significant differences ($p < 0.05$) between Col-0 WT and *efr* mutants are indicated.

Figure 5. EFR suppresses genome editing efficiency

Agrobacterium GV3101 carrying a binary vector encoding a base editor and a sgRNA was used for floral inoculation in Col-0 WT and *efr* mutants to assess genome editing

641 and stable transformation efficiencies. (a) A schematic diagram of the binary vector
642 structure for base editing and target gene information. (b) Genome editing efficiency
643 assessed by tribenuron resistant T1 plants with targeting the *ALS* Pro197 locus. (c)
644 Stable transformation efficiency evaluated by hygromycin resistance. Seeds are
645 collected from flowers that opened at 5-9 DPI. Data are mean ± SD, with *p*-values
646 calculated by Student's t-test between Col-0 WT and *efr* mutants. (d) Genome editing
647 efficiency assessed based on albino phenotype in T1 plants, resulting from by loss-of-
648 function mutations at locus *CLA1 and PDS3.* Statistically significant differences between
649 Col-0 WT and *efr* are indicated (*$p < 0.05$, **$p < 0.01$, chi-square analysis).

650

651 **Figure 6. Modification of *Agrobacterium* EF-Tu enhances transient gene**
652 **expression and genome editing efficiency but not stable T-DNA integration**
653 **efficiency**

654 The two engineered *Agrobacterium tufAB*$^{Pst4\text{-}15}$ strains, AS201 and AS202, were
655 assessed for its efficiency in transient expression, genome editing, and stable
656 transformation in comparison to the parental *Agrobacterium* GV3101.

657 (a) A schematic diagram illustrating the difference of *tufAB* sequences at amino acids
658 4th to 15th between *Agrobacterium* GV3101 and *Pseudomonas syringae* (*Pst*).

659 (b, c) Comparison of transient transformation efficiencies between the GV3101 WT and
660 two *tufAB*$^{Pst4\text{-}15}$ strains (AS201 and AS202) in *A. thaliana* seedlings by quantitative GUS
661 activity (b) GUS staining (c, scale bar =1 cm). Results are representative of three
662 independent experiments.

663 (d) Comparison of genome editing efficiency between the GV3101 WT and two
664 *tufAB*$^{Pst4\text{-}15}$ strains (AS201 and AS202) measured by the percentage of tribenuron-
665 resistant T1 plants (left) and number of edited T1 plants per three T0 plants (right).

666 (e) Comparison of stable transformation efficiency by the number of hygromycin-
667 resistant T1 plants per three T0 plants, with no significant differences between WT
668 GV3101 and the two *tufAB*$^{Pst4\text{-}15}$ strains (AS201 and AS202).

669 Seeds were collected from all flowers. Each data point represents biological replicates
670 from three independent experiments. All values are shown as mean ± SD, with *p*-values
671 calculated by Student's t-test.

672

673 **Figure 7. Sequencing-based screening of genome-edited plants**

674 (a) Workflow for screening genome-edited T1 plants from flowers that opened at 6 DPI.
675 Seeds were germinated in 1/2 MS medium with only supplemented with timentin to

676 suppress *Agrobacterium* growth without hygromycin selection. 10-day-old T1 plants
677 were analyzed by Sanger sequencing at the *ALS* or *CLA1* loci.

678 (b) The number of sequenced T1 plants and editing rates. †indicates the C to T editing
679 at Pro197 locus conferring tribenuron resistance. Statistically significant differences in
680 genome editing (GE) rates between *efr*-1 and WT Col-0 are indicated (*$p < 0.001$, chi-
681 square analysis).

682

683

684 **Figure S1. EFR-mediated immunity exerts negative impacts on ovule**
685 **development and RUBY-based transformation rate**

686 GV3101 carrying the 35S::RUBY construct was used for AMT-FI to assess RUBY-
687 based transformation efficiency and ovule abortion rate in Col-0 WT and *efr* mutants.
688 Siliques from flowers that opened at 5-9 DPI were analyzed to count the total number of
689 ovules, the number of developed ovules with or without RUBY signals, and the number
690 of abortive ovules with or without RUBY signals per silique.

691 (a) Daily RUBY-based transformation rate per silique. The percentage of RUBY-positive
692 ovules (including both developed and abortive ovules) per silique was calculate at each
693 DPI, as well as cumulatively across 5-9 DPI. Each data point represents the percentage
694 of RUBY-positive ovules per silique.

695 (b) Daily RUBY-based transformation rate of developed ovules per silique. The
696 percentage of RUBY-positive developed (non-abortive) ovules per silique was
697 measured at each DPI, as well as cumulatively across 5-9 DPIs. Each data point
698 represents the percentage of RUBY-positive developed ovules per silique.

699 (c) Daily ovule abortion rate per silique. The percentage of abortive ovules (including
700 both RUBY-positive and RUBY-negative) per silique was recorded at each DPI and
701 cumulatively across 5-9 DPI. Each data point represents the percentage of abortive
702 ovules per silique.

703 Data are shown in mean ± SD from three independent experiments, with *p*-values
704 calculated by Student's t-test between Col-0 WT and *efr* mutants.

705 Related to Figure 3.

706

707 **Figure S2. *Agrobacterium* infection and EFR-mediated immunity affect seed**
708 **outputs**

709 (a) Table showing seed number per silique from plants treated with infiltration medium
710 alone or with *Agrobacterium.* (b) Seed counts and germination rates following infiltration

711 medium alone (IM) or with *Agrobacterium* IM (IM + GV3101) treatments. Siliques were
712 collected from flowers that opened at 5–9 DPI. The total number of seeds and the
713 number of germinated seeds were compared between treatments. Data were collected
714 from two plants per genotype, except for *efr*-1 infected with GV3101, where data were
715 obtained from one plant. Data are shown as mean ± SD, with *p*-values calculated using
716 Student's *t*-test to compare Col-0 WT and *efr* mutants.

717

REFERENCES

Anand, A., Uppalapati, S.R., Ryu, C.M., Allen, S.N., Kang, L., Tang, Y. and Mysore, K.S. (2008) Salicylic acid and systemic acquired resistance play a role in attenuating crown gall disease caused by *Agrobacterium tumefaciens*. *Plant Physiol.* **146**, 703-715.

Angulo, J., Astin, C.P., Bauer, O., Blash, K.J., Bowen, N.M., Chukwudinma, N.J., DiNofrio, A.S., Faletti, D.O., Ghulam, A.M., Gusinde-Duffy, C.M., Horace, K.J., Ingram, A.M., Isaack, K.E., Jeong, G., Kiser, R.J., Kobylanski, J.S., Long, M.R., Manning, G.A., Morales, J.M., Nguyen, K.H., Pham, R.T., Phillips, M.H., Reel, T.W., Seo, J.E., Vo, H.D., Wukoson, A.M., Yeary, K.A., Zheng, G.Y. and Lukowitz, W. (2023) CRISPR/Cas9 mutagenesis of the *Arabidopsis* GROWTH-REGULATING FACTOR (GRF) gene family. *Front. Genome Ed.* **5**, 1251557.

Baud, S., Boutin, J.-P., Miquel, M., Lepiniec, L. and Rochat, C. (2002) An integrated overview of seed development in *Arabidopsis thaliana* ecotype WS. *Plant Physiol. Biochem.* **40**, 151-160.

Bechtold, N., Jaudeau, B., Jolivet, S., Maba, B., Vezon, D., Voisin, R. and Pelletier, G. (2000) The maternal chromosome set is the target of the T-DNA in the in planta transformation of *Arabidopsis thaliana*. *Genetics* **155**, 1875-1887.

Bechtold, N., Jolivet, S., Voisin, R. and Pelletier, G. (2003) The endosperm and the embryo of *Arabidopsis thaliana* are independently transformed through infiltration by *Agrobacterium tumefaciens*. *Transgenic Res.* **12**, 509-517.

Bélanger, J.G., Copley, T.R., Hoyos-Villegas, V., Charron, J.B. and O'Donoughue, L. (2024) A comprehensive review of in planta stable transformation strategies. *Plant Methods* **20**, 79.

Bevan, M. (1984) Binary *Agrobacterium* vectors for plant transformation. *Nucleic Acids Res.* **12**, 8711-8721.

Boschi, F., Schvartzman, C., Murchio, S., Ferreira, V., Siri, M.I., Galván, G.A., Smoker, M., Stransfeld, L., Zipfel, C., Vilaró, F.L. and Dalla-Rizza, M. (2017) Enhanced bacterial wilt resistance in potato through expression of *Arabidopsis* EFR and introgression of quantitative resistance from *Solanum commersonii*. *Front. Plant Sci.* **8**, 1642.

Chen, Y., Wang, Z., Ni, H., Xu, Y., Chen, Q. and Jiang, L. (2017) CRISPR/Cas9-mediated base-editing system efficiently generates gain-of-function mutations in *Arabidopsis*. *Sci. China Life Sci.* **60**, 520-523.

Clough, S.J. and Bent, A.F. (1998) Floral dip: a simplified method for *Agrobacterium*-mediated transformation of *Arabidopsis thaliana*. *Plant J.* **16**, 735-743.

Desfeux, C., Clough, S.J. and Bent, A.F. (2000) Female reproductive tissues are the primary target of *Agrobacterium*-mediated transformation by the *Arabidopsis* floral-dip method. *Plant Physiol.* **123**, 895-904.

Dickinson, L., Yuan, W., LeBlanc, C., Thomson, G., Wang, S. and Jacob, Y. (2023) Regulation of gene editing using T-DNA concatenation. *Nat. Plants* **9**, 1398-1408.

Dodds, P.N., Chen, J. and Outram, M.A. (2024) Pathogen perception and signaling in plant immunity. *Plant Cell* **36**, 1465-1481.

Fan, L., Fröhlich, K., Melzer, E., Pruitt, R.N., Albert, I., Zhang, L., Joe, A., Hua, C., Song, Y., Albert, M., Kim, S.T., Weigel, D., Zipfel, C., Chae, E., Gust, A.A. and Nürnberger, T. (2022) Genotyping-by-sequencing-based identification of *Arabidopsis* pattern recognition receptor RLP32 recognizing proteobacterial translation initiation factor IF1. *Nat. Commun.* **13**, 1294.

Fürst, U., Zeng, Y., Albert, M., Witte, A.K., Fliegmann, J. and Felix, G. (2020) Perception of *Agrobacterium tumefaciens* flagellin by FLS2(XL) confers resistance to crown gall disease. *Nat. Plants* **6**, 22-27.

Gelvin, S.B. (2003) *Agrobacterium*-mediated plant transformation: the biology behind the "gene-jockeying" tool. *Microbiol. Mol. Biol. Rev.* **67**, 16-37, table of contents.

764 Hooykaas, P.J.J. (2023) The Ti plasmid, driver of *Agrobacterium* pathogenesis. *Phytopathology* **113**, 594-
765 604.
766 Huang, T.-K. and Puchta, H. (2021) Novel CRISPR/Cas applications in plants: from prime editing to
767 chromosome engineering. *Transgenic Res.* **30**, 529-549.
768 Hwang, H.H., Yu, M. and Lai, E.M. (2017) *Agrobacterium*-mediated plant transformation: biology and
769 applications. *Arabidopsis Book* **15**, e0186.
770 Kado, C.I. and Heskett, M.G. (1970) Selective media for isolation of *Agrobacterium*, *Corynebacterium*,
771 *Erwinia*, *Pseudomonas*, and *Xanthomonas*. *Phytopathology* **60**, 969-976.
772 Kiselev, K.V., Aleynova, O.A., Ogneva, Z.V., Suprun, A.R. and Dubrovina, A.S. (2021) 35S promoter-driven
773 transgenes are variably expressed in different organs of *Arabidopsis thaliana* and in response to
774 abiotic stress. *Mol. Biol. Rep.* **48**, 2235-2241.
775 Kunwar, S., Iriarte, F., Fan, Q., Evaristo da Silva, E., Ritchie, L., Nguyen, N.S., Freeman, J.H., Stall, R.E.,
776 Jones, J.B., Minsavage, G.V., Colee, J., Scott, J.W., Vallad, G.E., Zipfel, C., Horvath, D., Westwood,
777 J., Hutton, S.F. and Paret, M.L. (2018) Transgenic expression of EFR and Bs2 genes for field
778 management of bacterial wilt and bacterial spot of Tomato. *Phytopathology* **108**, 1402-1411.
779 Lacroix, B. and Citovsky, V. (2019) Pathways of DNA transfer to plants from *Agrobacterium tumefaciens*
780 and related bacterial species. *Annu. Rev. Phytopathol.* **57**, 231-251.
781 Liu, D., Xuan, S., Prichard, L.E., Donahue, L.I., Pan, C., Nagalakshmi, U., Ellison, E.E., Starker, C.G., Dinesh-
782 Kumar, S.P., Qi, Y. and Voytas, D.F. (2022) Heritable base-editing in *Arabidopsis* using RNA viral
783 vectors. *Plant Physiol.* **189**, 1920-1924.
784 Lopez-Agudelo, J.C., Goh, F.-J., Tchabashvili, S., Huang, Y.-S., Huang, C.-Y., Lee, K.-T., Wang, Y.-C., Wu, Y.,
785 Chang, H.-X., Kuo, C.-H., Lai, E.-M. and Wu, C.-H. (2024) *Rhizobium rhizogenes* A4-derived strains
786 mediate hyper-efficient transient gene expression in *Nicotiana benthamiana* and other
787 solanaceous plants. *Plant Biotechnol. J.*
788 Lu, F., Wang, H., Wang, S., Jiang, W., Shan, C., Li, B., Yang, J., Zhang, S. and Sun, W. (2015) Enhancement
789 of innate immune system in monocot rice by transferring the dicotyledonous elongation factor
790 Tu receptor EFR. *J. Integr. Plant Biol.* **57**, 641-652.
791 Mysore, K.S., Kumar, C.T. and Gelvin, S.B. (2000) *Arabidopsis* ecotypes and mutants that are recalcitrant
792 to *Agrobacterium* root transformation are susceptible to germ-line transformation. *Plant J.* **21**,
793 9-16.
794 Nam, J., Matthysse, A.G. and Gelvin, S.B. (1997) Differences in susceptibility of *Arabidopsis* ecotypes to
795 crown gall disease may result from a deficiency in T-DNA integration. *Plant Cell* **9**, 317-333.
796 Nishizawa-Yokoi, A., Saika, H., Hara, N., Lee, L.Y., Toki, S. and Gelvin, S.B. (2021) *Agrobacterium* T-DNA
797 integration in somatic cells does not require the activity of DNA polymerase θ. *New Phytol.* **229**,
798 2859-2872.
799 Piazza, S., Campa, M., Pompili, V., Costa, L.D., Salvagnin, U., Nekrasov, V., Zipfel, C. and Malnoy, M.
800 (2021) The *Arabidopsis* pattern recognition receptor EFR enhances fire blight resistance in apple.
801 *Hortic. Res.* **8**.
802 Pixley, K.V., Falck-Zepeda, J.B., Paarlberg, R.L., Phillips, P.W.B., Slamet-Loedin, I.H., Dhugga, K.S.,
803 Campos, H. and Gutterson, N. (2022) Genome-edited crops for improved food security of
804 smallholder farmers. *Nat. Genet.* **54**, 364-367.
805 Raman, V., Rojas, C.M., Vasudevan, B., Dunning, K., Kolape, J., Oh, S., Yun, J., Yang, L., Li, G., Pant, B.D.,
806 Jiang, Q. and Mysore, K.S. (2022) *Agrobacterium* expressing a type III secretion system delivers
807 *Pseudomonas* effectors into plant cells to enhance transformation. *Nat. Commun.* **13**, 2581.
808 Ren, Q., Sretenovic, S., Liu, G., Zhong, Z., Wang, J., Huang, L., Tang, X., Guo, Y., Liu, L., Wu, Y., Zhou, J.,
809 Zhao, Y., Yang, H., He, Y., Liu, S., Yin, D., Mayorga, R., Zheng, X., Zhang, T., Qi, Y. and Zhang, Y.
810 (2021) Improved plant cytosine base editors with high editing activity, purity, and specificity.
811 *Plant Biotechnol. J.* **19**, 2052-2068.

812 Roca Paixao, J.F. and Deleris, A. (2024) Epigenetic control of T-DNA during transgenesis and
813 pathogenesis. *Plant Physiol.* **197**.
814 Saur, I.M., Kadota, Y., Sklenar, J., Holton, N.J., Smakowska, E., Belkhadir, Y., Zipfel, C. and Rathjen, J.P.
815 (2016) NbCSPR underlies age-dependent immune responses to bacterial cold shock protein in
816 *Nicotiana benthamiana*. *Proc. Natl. Acad. Sci. U. S. A.* **113**, 3389-3394.
817 Schwessinger, B., Bahar, O., Thomas, N., Holton, N., Nekrasov, V., Ruan, D., Canlas, P.E., Daudi, A.,
818 Petzold, C.J., Singan, V.R., Kuo, R., Chovatia, M., Daum, C., Heazlewood, J.L., Zipfel, C. and
819 Ronald, P.C. (2015) Transgenic expression of the dicotyledonous pattern recognition receptor
820 EFR in rice leads to ligand-dependent activation of defense responses. *PLoS Pathog.* **11**,
821 e1004809.
822 Shih, P.Y., Chou, S.J., Müller, C., Halkier, B.A., Deeken, R. and Lai, E.M. (2018) Differential roles of
823 glucosinolates and camalexin at different stages of *Agrobacterium*-mediated transformation.
824 *Mol. Plant Pathol.* **19**, 1956-1970.
825 Steinert, J., Schiml, S., Fauser, F. and Puchta, H. (2015) Highly efficient heritable plant genome
826 engineering using Cas9 orthologues from *Streptococcus thermophilus* and *Staphylococcus*
827 *aureus*. *Plant J.* **84**, 1295-1305.
828 Suzuki, K., Tanaka, K., Yamamoto, S., Kiyokawa, K., Moriguchi, K. and Yoshida, K. (2009) Ti and Ri
829 plasmids. In: *Microbial Megaplasmids* (Schwartz, E. ed) pp. 133-147. Berlin, Heidelberg: Springer
830 Berlin Heidelberg.
831 Szarzanowicz, M.J., Waldburger, L.M., Busche, M., Geiselman, G.M., Kirkpatrick, L.D., Kehl, A.J., Tahmin,
832 C., Kuo, R.C., McCauley, J., Pannu, H., Cui, R., Liu, S., Hillson, N.J., Brunkard, J.O., Keasling, J.D.,
833 Gladden, J.M., Thompson, M.G. and Shih, P.M. (2024) Binary vector copy number engineering
834 improves *Agrobacterium*-mediated transformation. *Nat. Biotechnol.*
835 Tiwari, M., Mishra, A.K. and Chakrabarty, D. (2022) *Agrobacterium*-mediated gene transfer: recent
836 advancements and layered immunity in plants. *Planta* **256**, 37.
837 van Kregten, M., de Pater, S., Romeijn, R., van Schendel, R., Hooykaas, P.J. and Tijsterman, M. (2016) T-
838 DNA integration in plants results from polymerase-θ-mediated DNA repair. *Nat. Plants* **2**, 16164.
839 van Tol, N., van Schendel, R., Bos, A., van Kregten, M., de Pater, S., Hooykaas, P.J.J. and Tijsterman, M.
840 (2022) Gene targeting in polymerase theta-deficient *Arabidopsis thaliana*. *Plant J.* **109**, 112-125.
841 Wang, Y.-C., Yu, M., Shih, P.-Y., Wu, H.-Y. and Lai, E.-M. (2018) Stable pH suppresses defense signaling
842 and is the key to enhance *Agrobacterium*-mediated transient expression in *Arabidopsis*
843 seedlings. *Sci. Rep.* **8**, 17071.
844 Wang, Z.-P., Xing, H.-L., Dong, L., Zhang, H.-Y., Han, C.-Y., Wang, X.-C. and Chen, Q.-J. (2015) Egg cell-
845 specific promoter-controlled CRISPR/Cas9 efficiently generates homozygous mutants for
846 multiple target genes in *Arabidopsis* in a single generation. *Genome Biol.* **16**, 144.
847 Weisberg, A.J. and Chang, J.H. (2023) Mobile genetic element flexibility as an underlying principle to
848 bacterial evolution. *Annu. Rev. Microbiol.* **77**, 603-624.
849 Wu, H.-Y., Liu, K.-H., Wang, Y.-C., Wu, J.-F., Chiu, W.-L., Chen, C.-Y., Wu, S.-H., Sheen, J. and Lai, E.-M.
850 (2014) AGROBEST: an efficient *Agrobacterium*-mediated transient expression method for
851 versatile gene function analyses in *Arabidopsis* seedlings. *Plant Methods* **10**, 19.
852 Yang, F., Li, G., Felix, G., Albert, M. and Guo, M. (2023) Engineered *Agrobacterium* improves
853 transformation by mitigating plant immunity detection. *New Phytol.* **237**, 2493-2504.
854 Ye, G.N., Stone, D., Pang, S.Z., Creely, W., Gonzalez, K. and Hinchee, M. (1999) *Arabidopsis* ovule is the
855 target for *Agrobacterium* in planta vacuum infiltration transformation. *Plant J.* **19**, 249-257.
856 Yu, M., Wang, Y.C., Huang, C.J., Ma, L.S. and Lai, E.M. (2021) *Agrobacterium tumefaciens* deploys a
857 versatile antibacterial strategy to increase its competitiveness. *J. Bacteriol.* **203**.

858 Zipfel, C., Kunze, G., Chinchilla, D., Caniard, A., Jones, J.D.G., Boller, T. and Felix, G. (2006) Perception of
859 the bacterial PAMP EF-Tu by the receptor EFR restricts *Agrobacterium*-mediated transformation.
860 *Cell* **125**, 749-760.

861

Figure 1

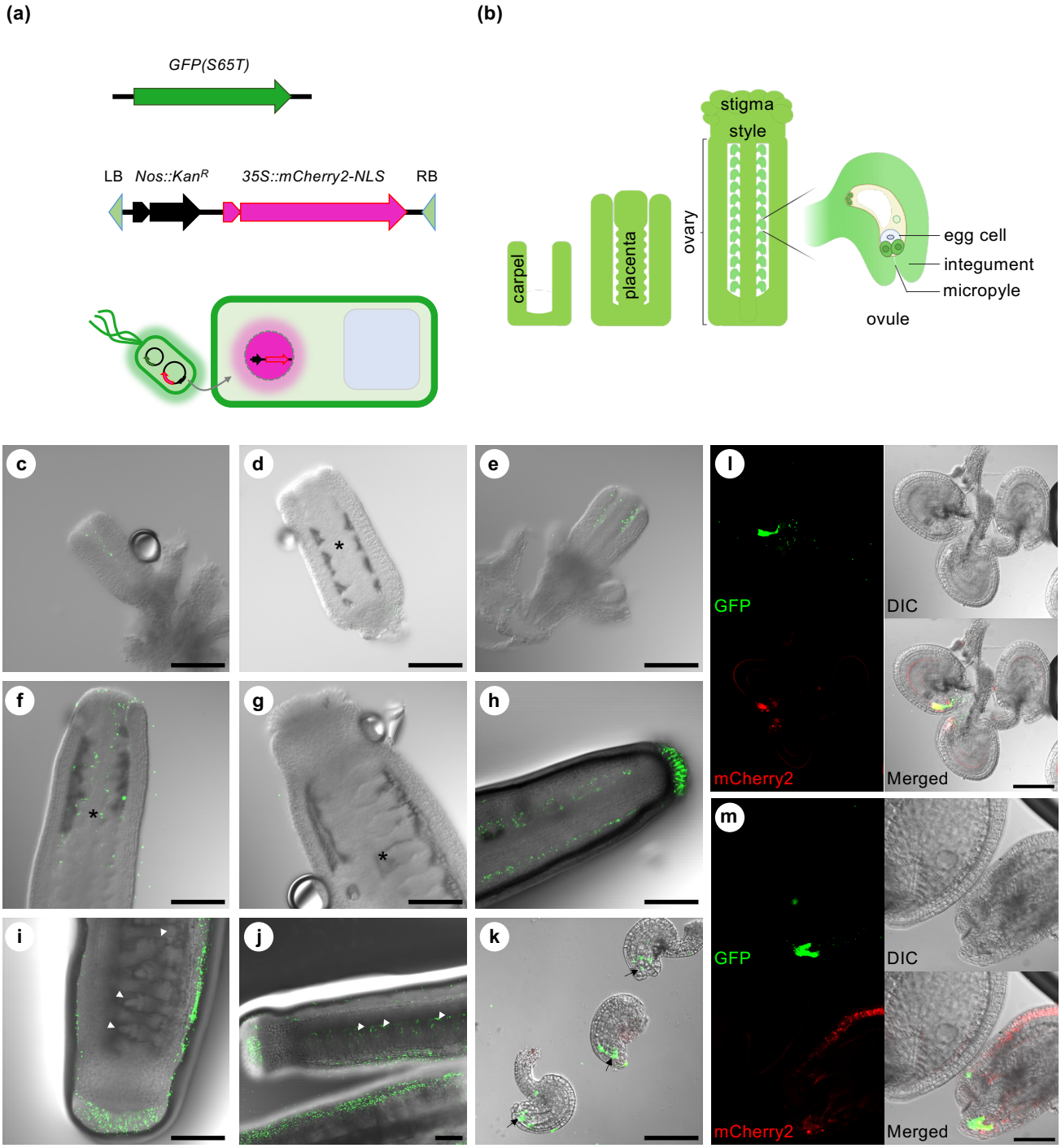

Figure 1. *Agrobacterium* enter open gynoecium within 1 hour but transformation events occur in open flowers after 5 days post inoculation

Agrobacterium GV3101 carrying pRL662-eGFP(S65T))/Spe^R and the binary vector 35S::mCherry2-NLS was used for floral inoculation on *Arabidopsis thaliana* Col-0 to visualize *Agrobacterium* localization and transformation events (a). Schematic illustration of the structure and development of gynoecium from early to mature stage with stigma, style, ovary containing ovules (b).

After 1 hour post-inoculation (HPI), *Agrobacterium* cells had already entered the locule of developing gynoecium (c) but were absent in later-stage gynoecia containing developed placenta tissue (d). Between 6-9 HPI, more *Agrobacterium* cells were observed in the locule (e), even at it began to close (f). No agrobacteria were detected in fully closed gynoecia (g).

At 1 day post-inoculation (DPI), *Agrobacterium* cells were detected in young closed ovaries (h) but not in older ovaries undergoing ovule development (i). At 3 DPI (j), *Agrobacterium* cells persisted in ovaries at late developmental stages. By 5 DPI, *Agrobacterium* cells were enriched around the micropyle (arrow) (k), though no mCherry2 signal was detected. At floral open stage after 6 DPI, *Agrobacterium* accumulated around the micropyle, and mCherry2 signal became visible (l and m).

Asterisks (*) indicate placenta tissue; arrowheads denote developing ovule; arrows indicate micropyle. Panels (a to k) were merged channel images; panels (l and m) show GFP, mCherry2, DIC and merged views. Scale bar= 100 µm.

Figure 2

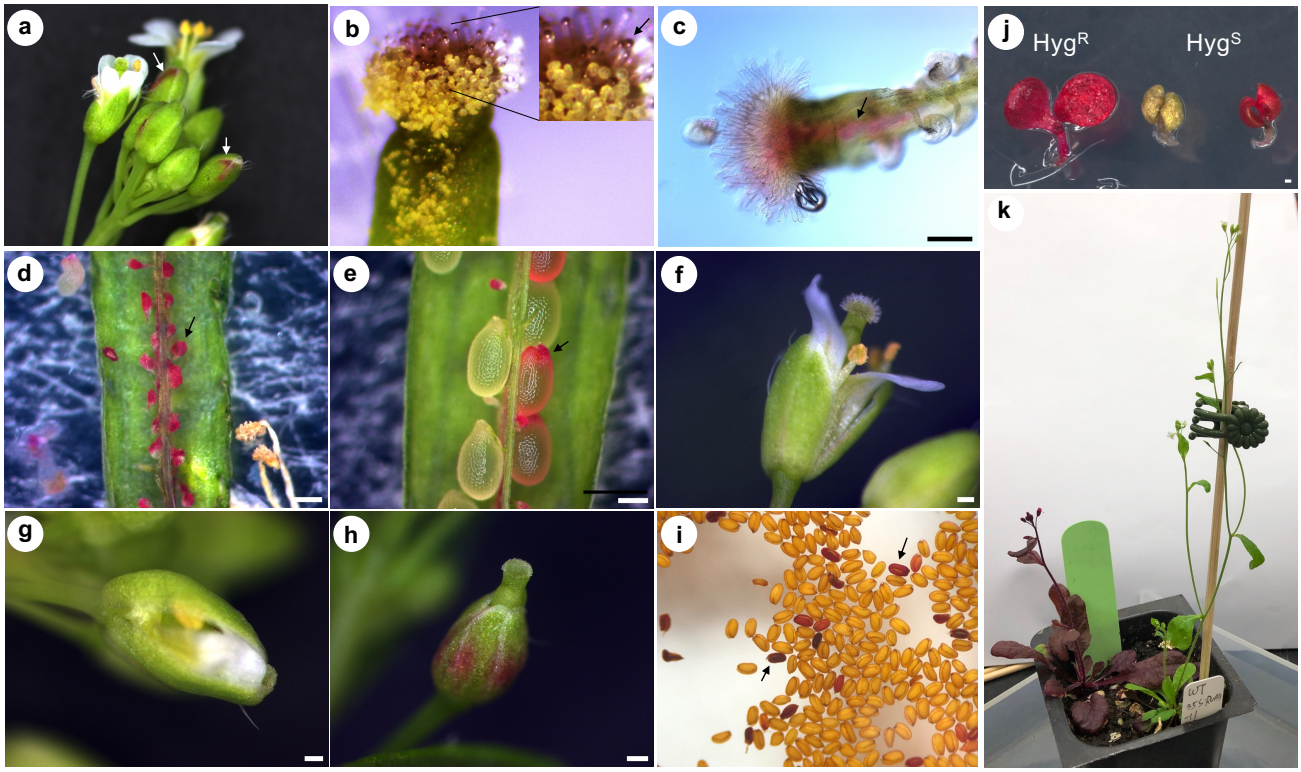

Figure 2. RUBY marker revealed transformation events in floral organs and female tissues

RUBY signals were observed in flowers (a), specifically on the stigma but not on pollen grains (b), and in the transmitting tissue (c). In siliques, RUBY expression was detected in both abortive (d) and developing ovules (e).

Flower morphology after AMT-FI ranged from normal open flowers (f) to partially open flowers (g), and flowers with only gynoecia emerging from sepals (h), all with visible RUBY signals.

RUBY signal intensity varied among seeds (i) and plants (j, k). (j) At the seedling stage, hygromycin resistant (Hyg^R) and RUBY-positive seedling (left), non-transgenic seedling (middle), and RUBY-positive but hygromycin sensitive (Hyg^S) seedling (right) were observed. (k) Transgenic T1 plants with variable RUBY expression patterns from strong whole-plant expression to undetectable signal. Scale bar = 200 μm.

Figure 3

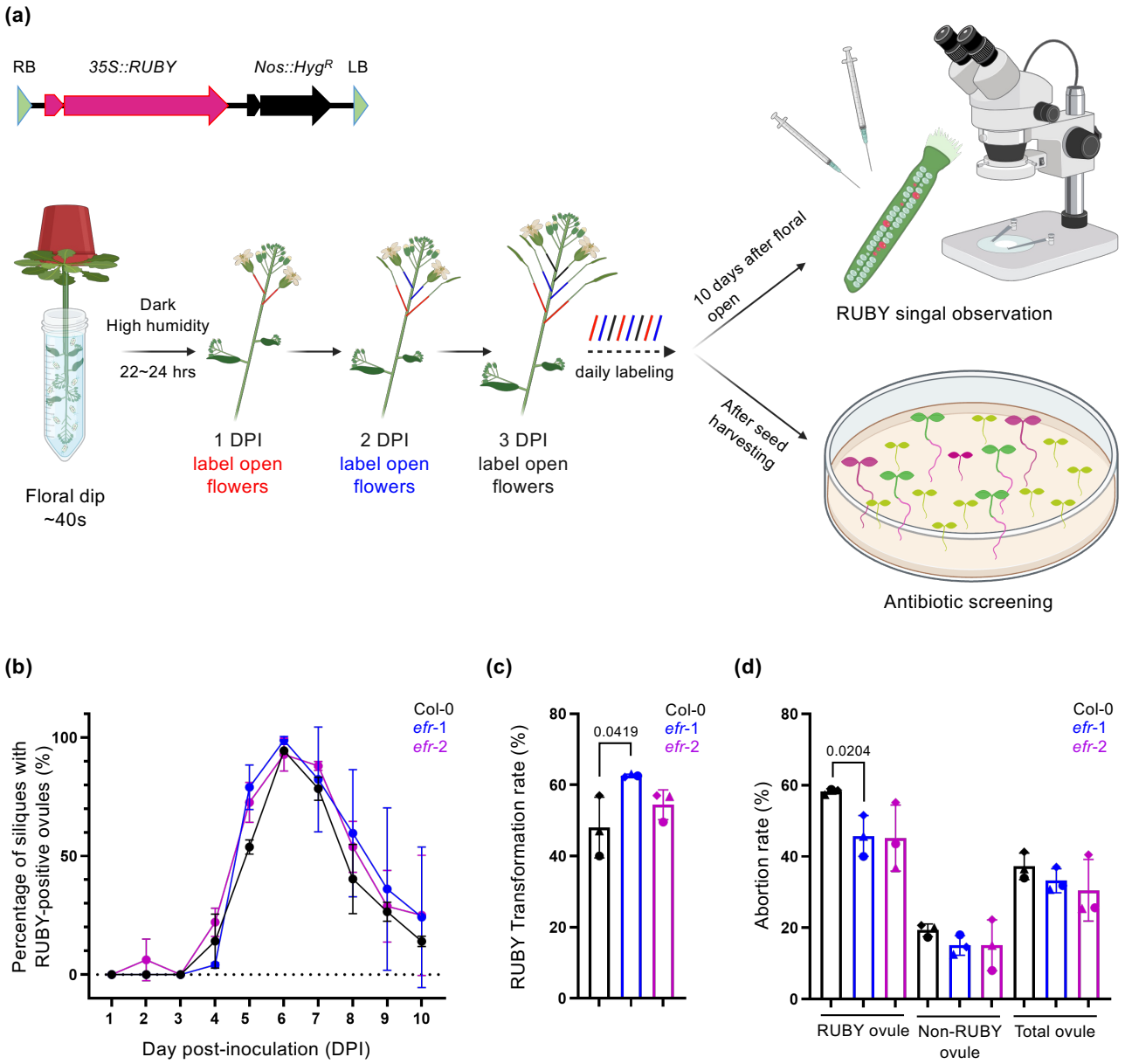

Figure 3. *Agrobacterium* infection and EFR-mediated immunity exert negative impacts on ovule development

(a) Experimental design: a schematic diagram illustrates the 35S::RUBY construct and experimental workflow. Transformation efficiency was evaluated based on the presence of RUBY-positive ovules and hygromycin-resistant seedlings.

(b) Percentage of siliques with RUBY-positive ovules recorded daily for Col-0 WT, *efr*-1, and *efr-2* from flowers that opened at 1-10 DPI. Data are mean ± SD of three biological replicates from representative of two independent experiments.

(c) RUBY-based transformation. Percentage of RUBY-positive ovules (include both developed and abortive ovules) per silique collected from flowers of Col-0 WT, *efr-1* and *efr-2* opened at 5-9 DPI was calculated (all data points shown in Fig. S2a). Data are mean ± SD of averaged percentage of RUBY-positive ovules from three independent experiments (circle, triangle and rhombus symbols). Statistically significant differences ($p < 0.05$) between Col-0 WT and efr mutants are indicated.

(d) Ovule abortion rate. The abortion rate of RUBY-positive, non-RUBY, and total ovules per silique collected from flowers of Col-0 WT, *efr*-1 and *efr*-2 opened at 5-9 DPI was calculated (all data points shown in Fig. S2c). Data are mean ± SD of averaged abortion rate from three independent experiments (circle, triangle and rhombus symbols). Statistically significant differences ($p < 0.05$) between Col-0 WT and efr mutants are indicated.

Figure 4

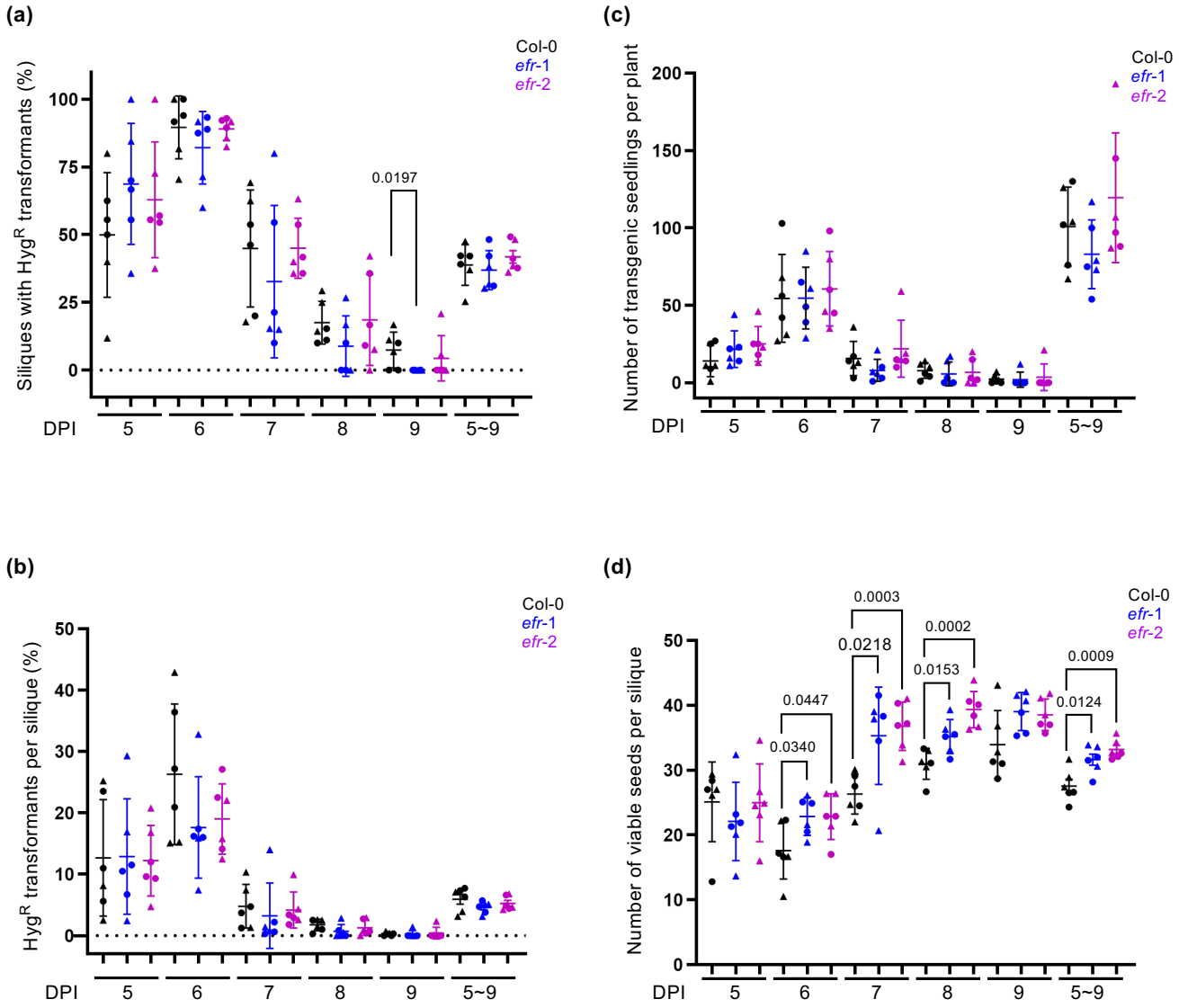

Figure 4. AMT events occur mainly in flowers opened at 5-9 DPI, peaking at 6 DPI

Siliques and seeds developed from flowers that opened at 5-9 DPI in Col-0 WT, *efr-1* and *efr-2* mutants were analyzed through hygromycin resistance screening (a, b, c) and viability (d). Data are (a) percentage of siliques containing Hyg^R transformants, (b) percentage of Hyg^R transformants per silique, (c) number of Hyg^R transformants per plant, and (d) number of viable seeds per silique. Data are mean ± SD of six biological replicates from two independent experiments (circle and triangle symbols). Statistically significant differences ($P < 0.05$) between Col-0 WT and *efr* mutants are indicated.

Figure 5

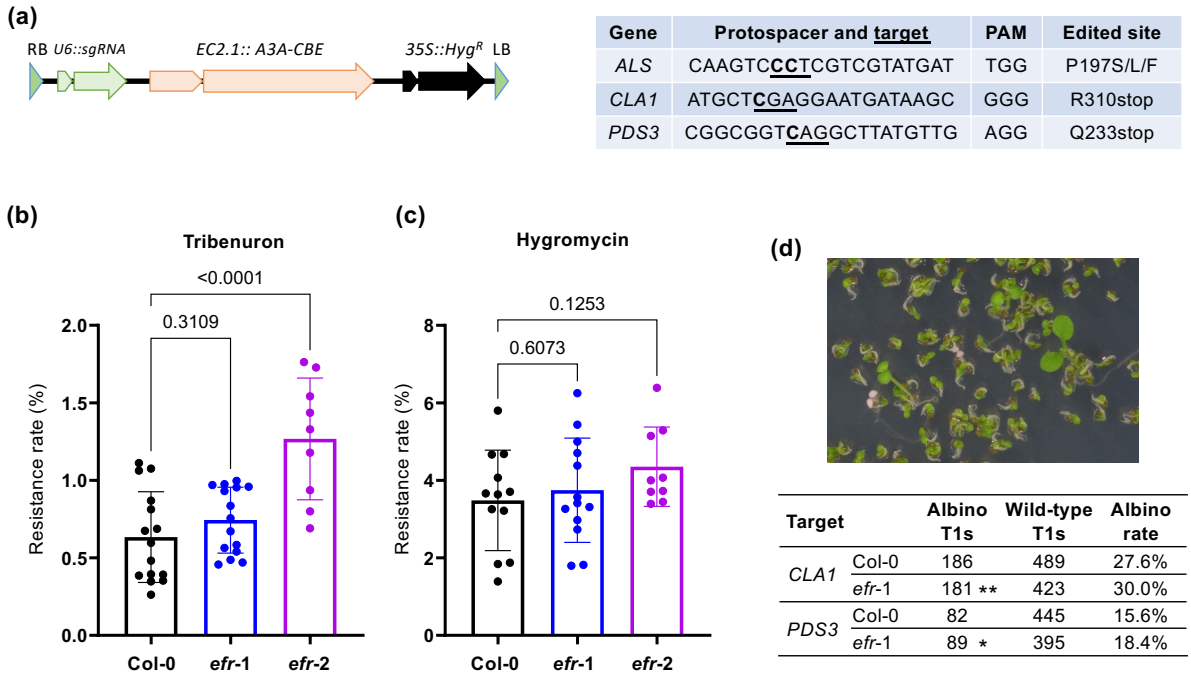

Gene	Protospacer and target	PAM	Edited site
ALS	CAAGTC**CC**TCGTCGTATGAT	TGG	P197S/L/F
CLA1	ATGCT**C**GAGGAATGATAAGC	GGG	R310stop
PDS3	CGGCGGT**C**AGGCTTATGTTG	AGG	Q233stop

Target		Albino T1s	Wild-type T1s	Albino rate
CLA1	Col-0	186	489	27.6%
	efr-1	181 **	423	30.0%
PDS3	Col-0	82	445	15.6%
	efr-1	89 *	395	18.4%

Figure 5. EFR suppresses genome editing efficiency

Agrobacterium GV3101 carrying a binary vector encoding a base editor and a sgRNA was used for floral inoculation in Col-0 WT and *efr* mutants to assess genome editing and stable transformation efficiencies. (a) A schematic diagram of the binary vector structure for base editing and target gene information. (b) Genome editing efficiency assessed by tribenuron resistant T1 plants with targeting the *ALS* Pro197 locus. (c) Stable transformation efficiency evaluated by hygromycin resistance. Seeds are collected from flowers that opened at 5-9 DPI. Data are mean ± SD, with p values calculated by Student's t-test between Col-0 WT and *efr* mutants. (d) Genome editing efficiency assessed based on albino phenotype in T1 plants, resulting from by loss-of-function mutations at locus *CLA1 and PDS3.* Statistically significant differences between Col-0 WT and *efr* are indicated (*p < 0.05, **p < 0.01, chi-square analysis).

Figure 6

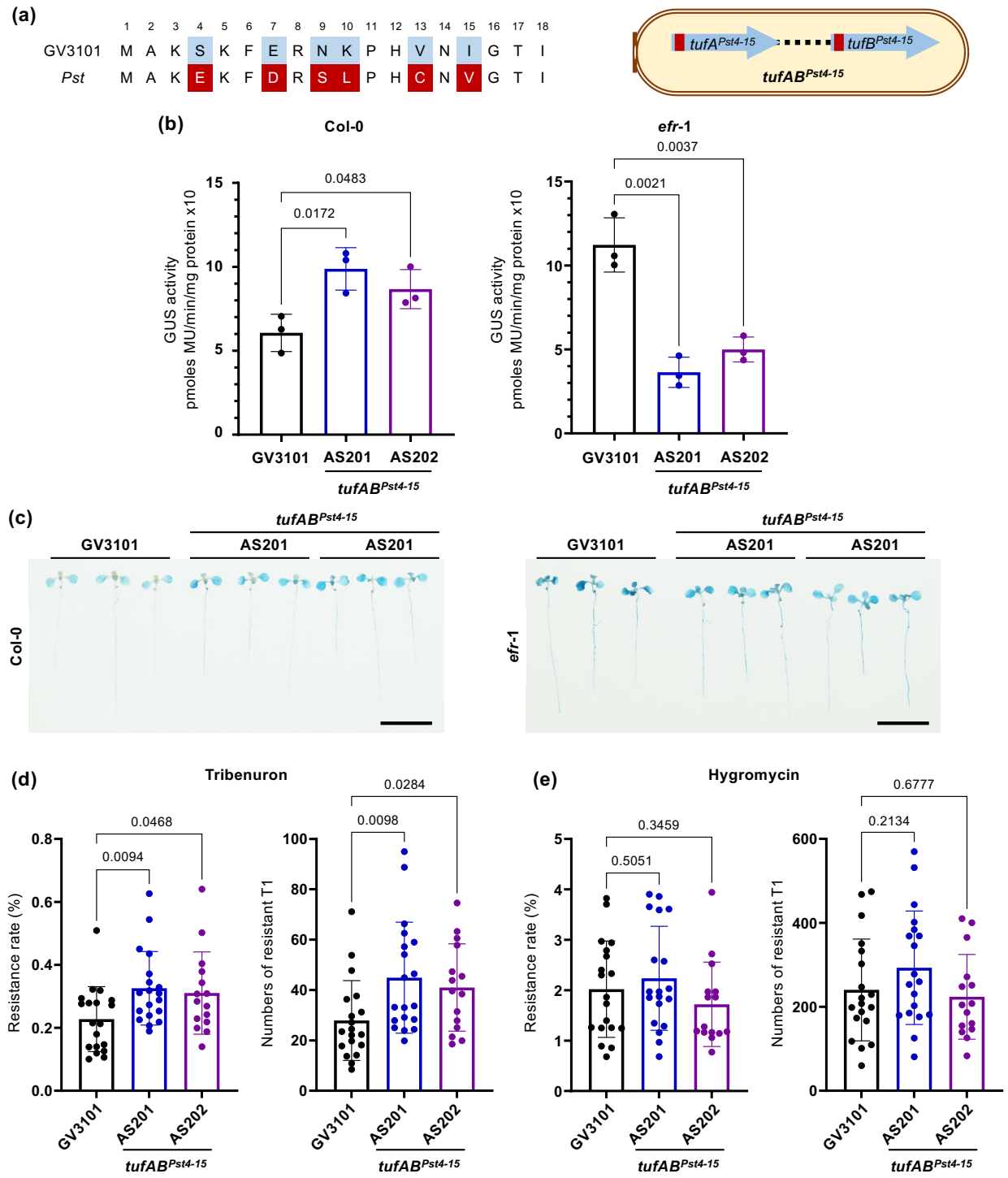

Figure 6. Modification of *Agrobacterium* EF-Tu enhances transient gene expression and genome editing efficiency but not stable T-DNA integration efficiency

The two engineered *Agrobacterium tufAB*$^{Pst4-15}$ strains were assessed for its efficiency in transient expression, genome editing, and stable transformation in comparison to the parental *Agrobacterium* GV3101.

(a) A schematic diagram illustratiing the difference of *tufAB* sequences at amino acids 4th to 15th between *Agrobacterium* GV3101 and *Pseudomonas syringae* (*Pst*.

(b, c) Comparison of transient transformation efficiencies between the GV3101 WT and two *tufAB*$^{Pst4-15}$ strains in *A. thaliana* seedlings by quantitative GUS activity (b) GUS staining (c, scale bar =1 cm). Results are representative of three independent experiments.

(d) Comparison of genome editing efficiency between the GV3101 WT and two *tufAB*$^{Pst4-15}$ strains measured by the percentage of tribenuron-resistant T1 plants (left) and number of edited T1 plants per three T0 plants (right).

(e) Comparison of stable transformation efficiency by the number of hygromycin-resistant T1 plants per three T0 plants, with no significant differences between WT GV3101 and the two *tufAB*$^{Pst4-15}$ strains.

Seeds were collected from flowers that opened at 5-9 DPI. Each data point represents biological replicates from three independent experiments. All values are shown as mean ± SD, with p values calculated by Student's t-test.

Figure 7

(a)

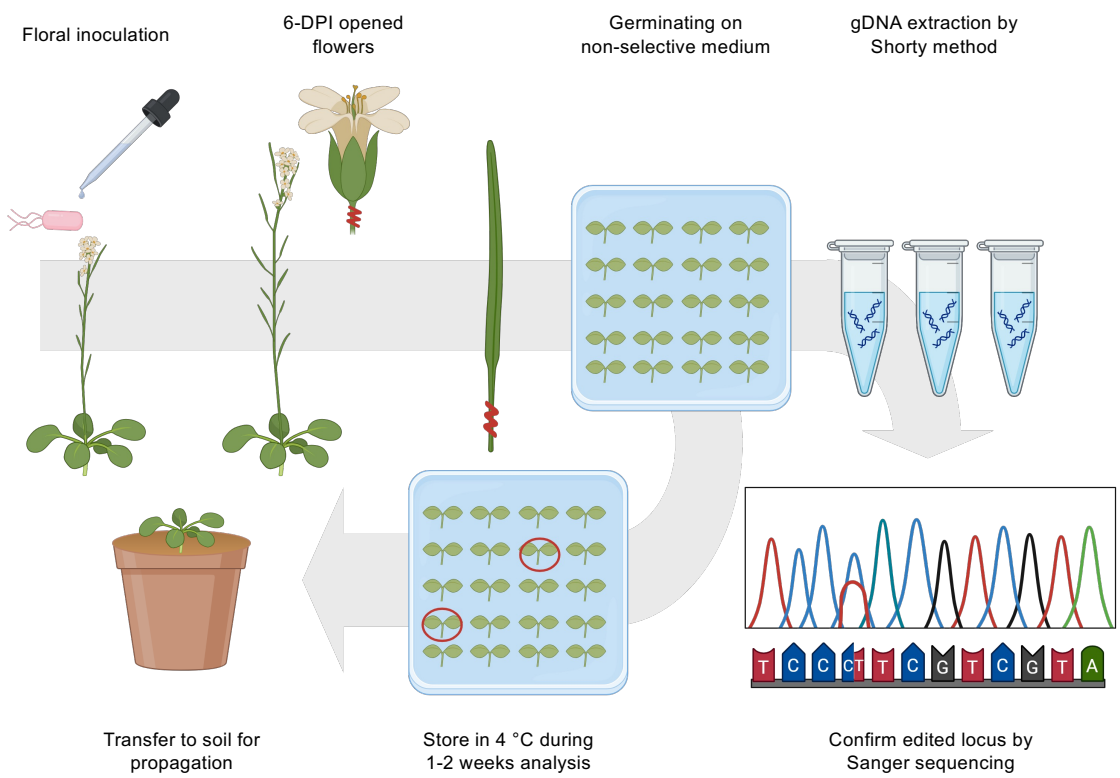

(b)

Plants	Col-0	*efr*-1	*efr*-2	Col-0	*efr*-1	*efr*-2	Col-0	Col-0
AMT-FI strain	GV3101	GV3101	GV3101	GV3101	GV3101	GV3101	GV3101	AS201
Target	*CLA1*	*CLA1*	*CLA1*	*CLA1*	*CLA1*	*CLA1*	*ALS*	*ALS*
Numbers of analyzed T1	212	188	236	64	63	64	94	93
GE phenotype	Albino			Sanger sequencing			Sanger sequencing†	
Numbers of edited T1	7	7	10	1	10*	3	1	2
GE rate	3.30%	3.72%	4.24%	1.56%	15.87%	4.69%	1.06%	2.15%

Figure 7. Sequencing-based screening of genome-edited plants

(a) Workflow for screening genome-edited T1 plants from flowers that opened at 6 DPI. Seeds were germinated in 1/2 MS medium with only supplemented with timentin to suppress *Agrobacterium* growth without hygromycin selection. 10-day-old T1 plants were analyzed by Sanger sequencing at the *ALS* or *PDS3* loci.

(b) The number of sequenced T1 plants and editing rates. †indicates the C to T editing at Pro197 locus conferring tribenuron resistance. Statistically significant differences in genome editing (GE) rates between *efr-1* and WT Col-0 are indicated (* $p < 0.001$ by Chi-Square test).

Supplemental figure 1

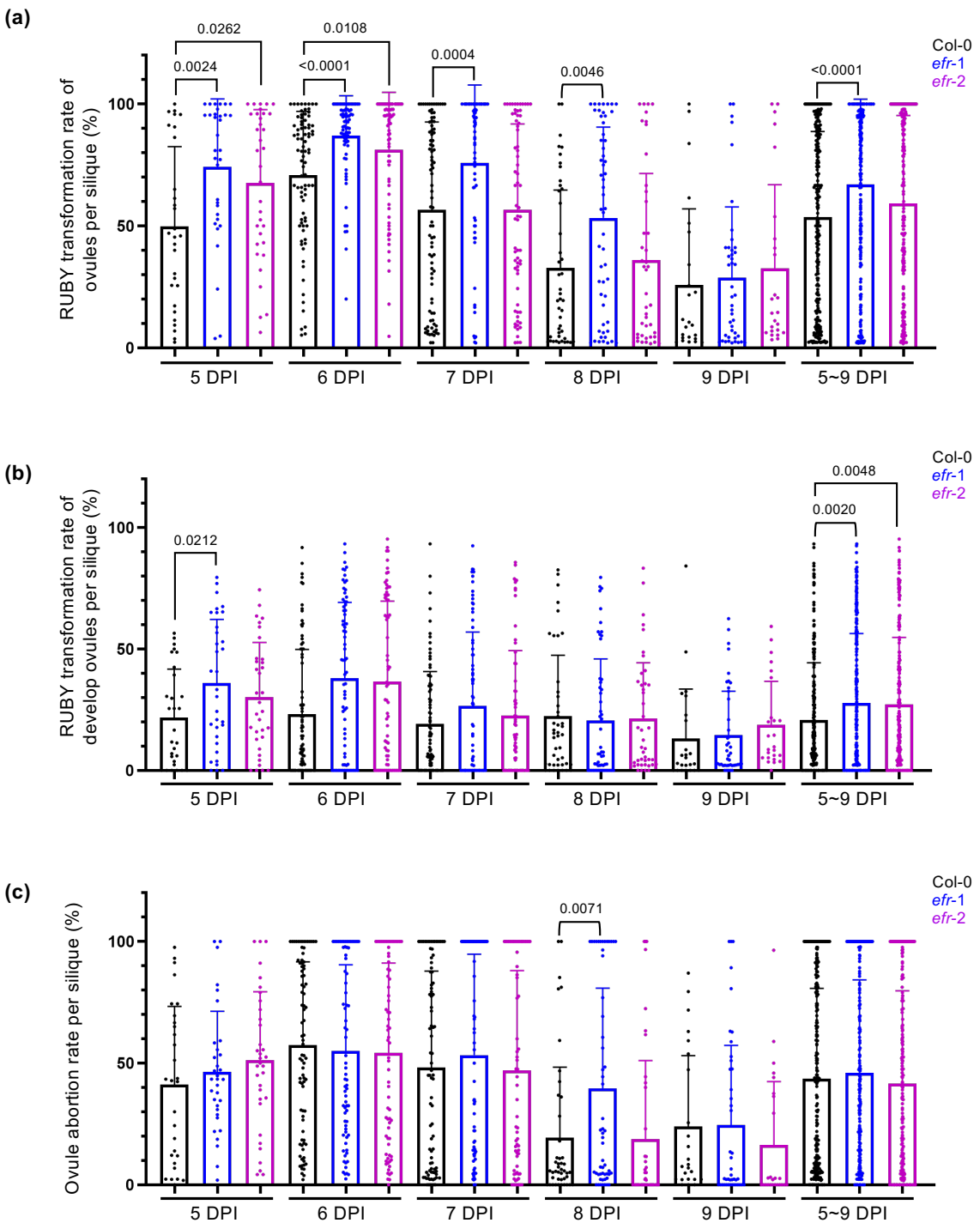

Figure S1. EFR-mediated immunity exerts negative impacts on ovule development and RUBY-based transformation rate

GV3101 carrying the 35S::RUBY construct was used for AMT-FI to assess RUBY-based transformation efficiency and ovule abortion rate in Col-0 WT and *efr* mutants. Siliques from flowers that opened at 5-9 DPI were analyzed to count the total number of ovules, the number of developed ovules with or without RUBY signals, and the number of abortive ovules with or without RUBY signals per silique. Related to Figure 3.

(a) Daily RUBY-based transformation rate per silique. The percentage of RUBY-positive ovules (including both developed and abortive ovules) per silique was calculate at each DPI, as well as cumulatively across 5-9 DPI. Each data point represents the percentage of RUBY-positive ovules per silique.

(b) Daily RUBY-based transformation rate of developed ovules per silique. The percentage of RUBY-positive developed (non-abortive) ovules per silique was measured at each DPI, as well as cumulatively across 5-9 DPIs. Each data point represents the percentage of RUBY-positive developed ovules per silique.

(c) Daily ovule abortion rate per silique. The percentage of abortive ovules (including both RUBY-positive and RUBY-negative) per silique was recorded at each DPI and cumulatively across 5-9 DPI. Each data point represents the percentage of abortive ovules per silique.

Data are shown in mean ± SD from three independent experiments, with p values calculated by Student's t-test between Col-0 WT and *efr* mutants.

Supplemental figure 2

(a)

Number of Developed Seeds						
Treatment	Infiltration Medium (IM)			IM+GV3101		
Genotype	Col-0	*efr*-1	*efr*-2	Col-0	*efr*-1	*efr*-2
Mean	35.6	42.7	44.5	29.4	37.4	40.6
SD	13.1	9.2	11.0	16.3	14.0	12.8
Number of Germinated Seeds (Germination Rate)						
Treatment	Infiltration Medium (IM)			IM+GV3101		
Genotype	Col-0	*efr*-1	*efr*-2	Col-0	*efr*-1	*efr*-2
Mean	35.5 (99.7%)	42.5 (99.5%)	44.3 (99.6%)	26.4 (89.8%)	34.4 (92.0%)	36.7 (90.4%)
SD	13.2	9.2	11.1	17.9	15.5	14.4

(b)

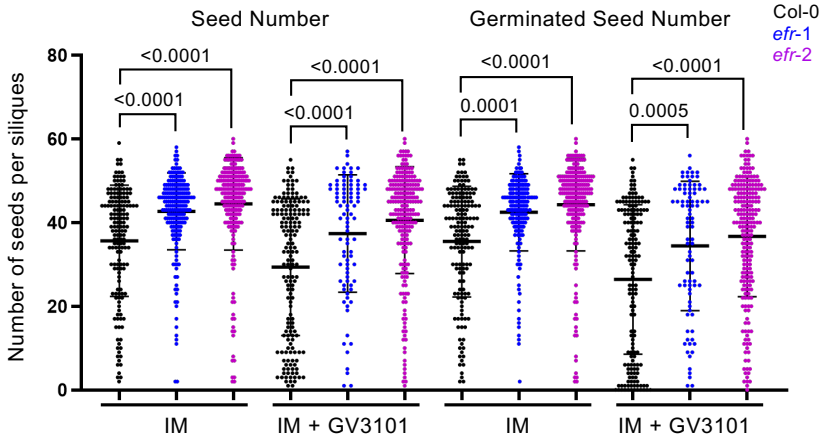

Figure S2. *Agrobacterium* infection and EFR-mediated immunity affect seed outputs

(a) Table showing seed number per silique from plants treated with infiltration medium alone or with *Agrobacterium.*
(b) Seed counts and germination rates following infiltration medium alone (IM) or with *Agrobacterium* IM (IM + GV3101) treatments. Siliques were collected from flowers that opened at 5–9 DPI. The total number of seeds and the number of germinated seeds were compared between treatments. Data were collected from two plants per genotype, except for *efr-1* infected with GV3101, where data were obtained from one plant. Data are shown as mean ± SD, with *p* values calculated using Student's *t*-test to compare *Col-0* WT and *efr* mutants.

Supplemental Table 1. Strain and Plasmid information

Lab collection #	***Agrobacterium* strain**/ Plasmid/ Antibiotics resistance	Characteristics	Source
EML485	**GV3101**/Rif^{R}Gen^R	GV3101 containing pMP90, which is pTiC58 derivative with T-DNA deletion and gentamicin resistance gene	Koncz and Schell, 1986
EML8561	**AS201**/ Rif^{R}Gen^R	GV3101::*tufAB*$^{Pst4-15}$ mutant by modifying *tufB* followed by *tufA*, with both genes encoding a chimeric EF-Tu with amino acids 4-15 from corresponding *Pst* EF-Tu	This study
EML8559	**AS202**/ Rif^{R}Gen^R	GV3101::*tufAB*$^{Pst4-15}$ mutant by modifying *tufA* followed by *tufB*, with both genes encoding a chimeric EF-Tu with amino acids 4-15 from corresponding *Pst* EF-Tu	This study
EML3375	pRL662-GFP(S65T)/ Gen^R	Broad host range plasmid confers gentamycin resistance and expression of GFP(S65T)	Yu et al., 2021
EML6428	pRL662-GFP(S65T)/Spe^R	Broad host range plasmid confers spectinomycin resistance and expression of GFP(S65T)	This study
EML6409	35S::RUBY/Spe^R	Binary vector carrying T-DNA expressing RUBY reporter and hygromycin resistance	Addgene#160908
EML6442	35S:mCherry2-NLS/Kan^R	Binary vector carrying T-DNA expressing mCherry2 florescent proteins	This study
EML8357	pA3A-CBECas9/Kan^R	Binary vector carrying T-DNA expressing base editor driven by egg-cell specific promoter	This study
EML8359	pA3A-CBECas9-Pro197/Kan^R	Binary vector carrying T-DNA expressing base editor targeting *ALS Pro197* locus	This study
EML8532	pA3A-CBECas9-CLA1/Kan^R	Binary vector carrying T-DNA expressing base editor targeting *CLA1*, generating early stop codon	This study
EML8533	pA3A-CBECas9-PDS3/Kan^R	Binary vector carrying T-DNA expressing base editor targeting *PDS3*, generating early stop codon	This study
EML121	pJQ200KS/Gen^R	Suicide plasmid contains *sacB* and Gm^R *traJ oriT* for the selection of double crossover events	Quandt and Hynes, 1993
EML8543	pEML041003/Kan^R	pJQ200KS derived suicide vector for gene replacement in *Agrobacterium*	This study
EML8552	pEML041003-tufAPst4-15/ Kan^R	Suicide vector for replacing 4th to 15th amino acids of *tufA*	This study
EML8553	pEML041003-tufBPst4-15/ Kan^R	Suicide vector for replacing 4th to 15th amino acids of *tufB*	This study

Gen^R, gentamycin resistance; Kan^R, kanamycin resistance; Rif^R, rifampicin resistance; Spe^R, spectinomycin resistance

Supplemental Table 2. Primer information

Primers	5' to 3' sequence	R.E. site	Source
Cloning of pRL662-GFP(S65T) with spectinomycin resistance			
Spe_F	GTCGATGTTTGATGTTATGGAGCAGCAACGATGGGGGAAGCGGTGATCGCCGAAGTATCG		This study
Spe_R	CGGGAAGCCGATCTCGGCTTGAACGAATTGTTATTTGCCGACTACCTTGGTGATCTCGCC		
662_F	CGATACTTCGGCGATCACCGCTTCCCCCATCGTTGCTGCTCCATAACATCAAACATCGAC		This study
662_R	GGCGAGATCACCAAGGTAGTCGGCAAATAACAATTCGTTCAAGCCGAGATCGGCTTCCCG		
Cloning of binary vector with 35S:mCherry2-NLS			
MC2-F	AAGGTCTCAAATGGTGAGTAAAGGAGAAGA	BsaI	This study
MC2-R	AAGGTCTCAAAGCTTAGGCGCCTACCTTTCTCTTCTTTTTTGGGCCTTTGTATAGTTCATCCATGCCACC	BsaI	
Cloning of protospacer			
Pro197-fw	ATTG CAAGTCCCTCGTCGTATGAT		Chen et al., 2017
Pro197-rv	AAAC ATCATACGACGAGGGACTTG		
CLA1-fw	ATTG ATGCTCGAGGAATGATAAGC		Liu et al., 2022
CLA1-rv	AAAC GCTTATCATTCCTCGAGCAT		
PDS3-fw	ATTG CGGCGGTCAGGCTTATGTTG		Liu et al., 2022
PDS3-rv	AAAC CAACATAAGCCTGACCGCCG		
Double crossover vector for cloning *tufA*$^{Pst4\text{-}15}$ and *tufB*$^{Pst4\text{-}15}$			
tufA-1f	TTGGTCTCAGGAGCACGATCTTGCGGATGC	BsaI	This study
tufA-1r	AGGTCTCGCCCTCCCGCATTGCAACGTCGGCACGATCGGTCACGTCG	BsaI	
tufA-2f	AGGTCTCGAGGGAACGATCAAATTTTTCCTTTGCCATGTGAATTGCTTCC	BsaI	
tufA-2r	AAGGTCTCGAGCGCAGTTCCGTCCACATCTTC	BsaI	
tufB-1f	TTGGTCTCAGGAGTTAGAGCTTGATTTCCACGTCAA	BsaI	
tufB-1r	AGGTCTCGCCCTCCCGCATTGCAACGTCGGCACGATCGGTCACGTCG	BsaI	
tufB-2f	AGGTCTCGAGGGAACGATCAAATTTTTCCTTTGCCATTAGTGGCTCTCC	BsaI	
tufB-2r	AAGGTCTCGAGCGTTCGAACCGAACCCTGA	BsaI	

References

Chen, Y., Wang, Z., Ni, H., Xu, Y., Chen, Q. and Jiang, L. (2017) CRISPR/Cas9-mediated base-editing system efficiently generates gain-of-function mutations in *Arabidopsis*. *Sci. China Life Sci.* **60**, 520-523.

Koncz, C. and Schell, J. (1986) The promoter of TL-DNA gene 5 controls the tissue-specific expression of chimaeric genes carried by a novel type of *Agrobacterium* binary vector. *Molec. Gen. Genet.* **204**, 383-396.

Liu, D., Xuan, S., Prichard, L.E., Donahue, L.I., Pan, C., Nagalakshmi, U., Ellison, E.E., Starker, C.G., Dinesh-Kumar, S.P., Qi, Y. and Voytas, D.F. (2022) Heritable base-editing in *Arabidopsis* using RNA viral vectors. *Plant Physiol.* **189**, 1920-1924.

Quandt, J. and Hynes, M.F. (1993) Versatile suicide vectors which allow direct selection for gene replacement in Gram-negative bacteria. *Gene* **127**, 15-21.

Yu M, Wang YC, Huang CJ, Ma LS, Lai EM. 2021. *Agrobacterium tumefaciens* deploys a versatile antibacterial strategy to increase its competitiveness. J Bacteriol 203:10.1128/jb. 00490-20.